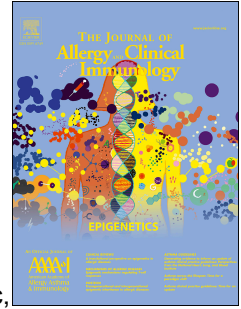


# Journal Pre-proof



BMP7 aberrantly induced in the psoriatic epidermis instructs inflammation-associated Langerhans cells

Izabela Borek, MSc, René Köffel, PhD, Julia Feichtinger, PhD, Melanie Spies, MD, Elisabeth Glitzner-Zeis, PhD, Mathias Hochgerner, MSc, Tommaso Sconocchia, MSc, Corinna Krump, PhD, Carmen Tam-Amersdorfer, BSc, Christina Passeger, MSc, Theresa Benezeder, MSc, Julia Tittes, MD, Anna Redl, MD, Clemens Painsi, MD, Gerhard G. Thallinger, PhD, Peter Wolf, MD, Georg Stary, MD, Maria Sibilia, PhD, Herbert Strobl, MD

PII: S0091-6749(19)31713-0

DOI: <https://doi.org/10.1016/j.jaci.2019.12.011>

Reference: YMAI 14312

To appear in: *Journal of Allergy and Clinical Immunology*

Received Date: 28 June 2019

Revised Date: 8 December 2019

Accepted Date: 13 December 2019

Please cite this article as: Borek I, Köffel R, Feichtinger J, Spies M, Glitzner-Zeis E, Hochgerner M, Sconocchia T, Krump C, Tam-Amersdorfer C, Passeger C, Benezeder T, Tittes J, Redl A, Painsi C, Thallinger GG, Wolf P, Stary G, Sibilia M, Strobl H, BMP7 aberrantly induced in the psoriatic epidermis instructs inflammation-associated Langerhans cells, *Journal of Allergy and Clinical Immunology* (2020), doi: <https://doi.org/10.1016/j.jaci.2019.12.011>.

This is a PDF file of an article that has undergone enhancements after acceptance, such as the addition of a cover page and metadata, and formatting for readability, but it is not yet the definitive version of record. This version will undergo additional copyediting, typesetting and review before it is published in its final form, but we are providing this version to give early visibility of the article. Please note that, during the production process, errors may be discovered which could affect the content, and all legal disclaimers that apply to the journal pertain.

© 2019 Published by Elsevier Inc. on behalf of the American Academy of Allergy, Asthma & Immunology.

# **BMP7 aberrantly induced in the psoriatic epidermis instructs inflammation-associated Langerhans cells**

Izabela Borek, MSc<sup>1</sup>, René Köffel, PhD<sup>2</sup>, Julia Feichtinger, PhD<sup>3</sup>, Melanie Spies, MD<sup>1</sup>, Elisabeth Glitzner-Zeis, PhD<sup>4</sup>, Mathias Hochgerner, MSc<sup>4</sup>, Tommaso Sconocchia, MSc<sup>1</sup>, Corinna Krump, PhD<sup>1</sup>, Carmen Tam-Amersdorfer, BSc<sup>1</sup>, Christina Passeger, MSc<sup>1</sup>, Theresa Benezeder, MSc<sup>5</sup>, Julia Tittes, MD<sup>6</sup>, Anna Redl, MD<sup>6</sup>, Clemens Painsi, MD<sup>7</sup>, Gerhard G Thallinger, PhD<sup>8,9</sup>, Peter Wolf, MD<sup>5</sup>, Georg Stary, MD<sup>6</sup>, Maria Sibilica, PhD<sup>4</sup>, Herbert Strobl, MD<sup>1\*</sup>

<sup>1</sup>Otto Loewi Research Center, Chair of Immunology and Pathophysiology, Medical University of Graz, Austria.

<sup>2</sup>Institute of Anatomy, University of Bern, Switzerland.

<sup>3</sup>Division of Cell Biology, Histology and Embryology, Gottfried Schatz Research Center for Cell Signaling, Metabolism and Aging, Medical University of Graz, Austria.

<sup>4</sup>Institute of Cancer Research, Department of Internal Medicine I, Medical University of Vienna, Austria.

<sup>5</sup>Department of Dermatology, Medical University of Graz, Austria.

<sup>6</sup>Division of Immunology, Allergy and Infectious Diseases, Department of Dermatology, Medical University of Vienna, Austria.

<sup>7</sup>Department of Dermatology, State Hospital Klagenfurt, Austria.

<sup>8</sup>Institute of Computational Biotechnology, Graz University of Technology, Austria.

<sup>9</sup>OMICS Center Graz, BioTechMed Graz, Austria.

## **Correspondence**

\*Herbert Strobl, Otto Loewi Research Center, Chair of Immunology and Pathophysiology, Medical University of Graz, Heinrichstrasse 31a, 8010 Graz, Austria, herbert.strobl@medunigraz.at

## **Key messages:**

- BMP7 instructs proliferating LCs with a psoriatic inflammation-associated phenotype
- The psoriatic epidermal niche is characterized by a BMP7/phospho-Smad1/5/8 signature
- In psoriatic patients reduction in epidermal BMP7 expression is associated with clinical improvement, and BMP signalling promotes psoriatic lesion formation in mice

**Capsule summary:** BMP signaling is functionally involved in the progression of psoriatic epidermal thickening, and serves as an instructive factor in self-renewal and differentiation of inflammation-associated LCs.

**Key words:** Langerhans cells, TGF- $\beta$  signaling, Psoriasis, BMP7

34 This work was supported by the Austrian Science Fund FWF (W1241) and the Medical University  
35 of Graz through the PhD Program Molecular Fundamentals of Inflammation (DK-MOLIN, to HS).  
36 Additional funding was obtained by FWF PhD program W1212 (to HS), FWF project P2572 (to HS),  
37 BioTechMed Graz (project “secretome”, to HS) and by the Austrian Ministry of Science, Research  
38 and Economy (HSRSM grant Omics Center Graz, to G.G.T.).

39 **The authors have declared that no conflict of interest exists.**

#### 40 **Abbreviations**

41	BG	Birbeck granules
42	BMP7	bone morphogenetic protein 7
43	DCs	dendritic cells
44	IDECs	inflammatory dendritic epidermal cells
45	KCs	keratinocytes
46	LCs	Langerhans cells
47	Nog	noggin
48	PASI	psoriasis area and severity index
49	PGN	peptidoglycan
50	TGF- $\beta$ 1	transforming growth factor beta 1
51	TLR	tool-like receptor

52

53

54

55

56

57

58

59

60

61 **Abstract**

62 **Background:** Epidermal hyperplasia represents a morphologic hallmark of psoriatic skin lesions.  
63 Langerhans cells (LCs) in the psoriatic epidermis engage with keratinocytes (KCs) in tight physical  
64 interactions; moreover, they induce T cell-mediated immune responses critical to psoriasis.

65 **Objective:** Epidermal factors in psoriasis pathogenesis remain poorly understood.

66 **Methods:** We phenotypically characterized BMP7-LCs vs. TGF- $\beta$ 1-LCs and analyzed their functional  
67 properties using flow cytometry, cell kinetic studies, co-culture with CD4 T-cells and cytokine  
68 measurements. Furthermore, immunohistology of healthy and psoriatic skin was performed.  
69 Additionally, *in vivo* experiments with Jun<sup>f/f</sup>JunB<sup>f/f</sup>K5cre<sup>ER</sup> mice were carried out to assess the role of  
70 BMP signaling in psoriatic skin inflammation.

71 **Results:** Here we identified a KC-derived signal, i.e. bone morphogenetic protein (BMP) signaling, to  
72 promote epidermal changes in psoriasis. Whereas BMP7 is strictly confined to the basal KC layer in  
73 the healthy skin, it is expressed at high levels throughout the lesional psoriatic epidermis. BMP7  
74 instructs precursor cells to differentiate into LCs that phenotypically resemble psoriatic LCs. These  
75 BMP7-LCs exhibit proliferative activity and increased sensitivity to bacterial stimulation. Moreover,  
76 aberrant high BMP signaling in the lesional epidermis is mediated by a KC intrinsic mechanism, as  
77 suggested from murine data and clinical outcome after topical anti-psoriatic treatment in human  
78 patients.

79 **Conclusion:** Our data indicate that available TGF- $\beta$  family members within the lesional psoriatic  
80 epidermis preferentially signal through the canonical BMP signaling cascade to instruct inflammatory-  
81 type LCs and to promote psoriatic epidermal changes. Targeting BMP signaling might allow to  
82 therapeutically interfere with cutaneous psoriatic manifestations.

83

84

85

86

87

88

89 **Introduction**

90 Langerhans cells (LCs) are a subset of dendritic cells (DCs) populating the epidermis and other  
91 squamous epithelia (1). They protect keratinocytes (KCs) from UV light-induced apoptosis (2) and  
92 contribute to skin homeostasis by maintaining proliferation of skin resident regulatory T cells (Tregs)  
93 (3,4). Psoriatic lesions are marked by epidermal thickening (acanthosis) due to impaired differentiation  
94 and enhanced proliferation of KCs (5). The human lesional psoriatic epidermis harbors two subsets of  
95 DCs: LCs and epithelial dendritic cells (DCs) that exhibit certain LC characteristics (6). These  
96 epidermal DCs are in physical contact with KCs and therefore might play critical roles in psoriasis-  
97 associated epidermal changes, as suggested from murine studies (7,8). *Vice versa*, psoriatic KCs might  
98 instruct precursors to adopt a disease-associated LC phenotype. Nevertheless, the functional roles of  
99 epidermal DCs and LCs remain poorly characterized as most published studies focused on dermal DCs  
100 (9). Following an inflammatory insult, endogenous LCs egress from the epidermis and are  
101 subsequently replenished from circulating monocytes (10–13), which acquire LC characteristics, but  
102 retain certain monocyte features (11). They seem to disappear after the resolution of inflammation and  
103 are subsequently replaced by proliferation of residual local LCs (14) or by immigrating non-monocyte,  
104 bone marrow-derived precursors (15). The epidermal microenvironment plays a key role in instructing  
105 LC differentiation (16), as highlighted by the observations that subsets of LCs from oral mucosa vs  
106 epidermis arise from distinct precursors; nevertheless, they exhibit a similar gene expression profile  
107 (17). *In vitro* studies revealed that besides monocytes, also human blood CD1c<sup>+</sup> DCs and CD14<sup>+</sup>  
108 dermal cells can differentiate into LCs (18–20). *In vitro*, keratinocyte-derived factors such as TGF- $\beta$ 1  
109 and BMP7 in cooperation with thymic stromal lymphopoietin (TSLP) and Notch ligands promote *in*  
110 *vitro* LC differentiation from human monocytes or monocyte-committed intermediates (21–23).  
111 However, unlike monocytes, CD1c<sup>+</sup> blood DCs do not require exogenous Notch ligand for LC  
112 differentiation (19). Belonging to the TGF- $\beta$  family, TGF- $\beta$ 1 and BMP7 both signal via BMP type-I  
113 receptor ALK3 to induce LC differentiation *in vitro* (24), and TGF- $\beta$ 1 can be replaced by BMP7 for  
114 instructing LC differentiation from CD1c<sup>+</sup> blood DCs and hematopoietic progenitor cells (19).  
115 Conversely, deletion of either TGF- $\beta$ 1, TGF- $\beta$ 1RII (25–27) or TGF- $\beta$  type I receptor ALK5 (28,29) in  
116 differentiated CD207<sup>+</sup> cells results in their emigration from the epidermis to the lymph nodes shortly

117 after birth. Moreover, ALK5 is dispensable for human LC differentiation *in vitro* (24). Whether or  
118 how local expression of TGF- $\beta$  ligands in the healthy and diseased epidermal microenvironment affect  
119 LC phenotype and function remains poorly understood. Considering the suspected functional  
120 importance of LCs in the maintenance of epidermal homeostasis, a better characterization of TGF- $\beta$   
121 family signaling in the psoriatic epidermis is of considerable medical relevance. Therefore, we here  
122 asked: What are the phenotypic and functional characteristics of BMP7-instructed LCs, and can we  
123 find such cells *in vivo* under pathophysiological conditions? We here identified BMP signaling to be  
124 functionally involved in the progression of psoriatic epidermal thickening, and to serve as an  
125 instructive factor in self-renewal and differentiation of inflammation-associated LCs.

126

127

128

129

130

131

132

133

134

135

136

137

138

139

140

141

142

143

**Materials and Methods*****In vitro* generation of CD34<sup>+</sup> progenitor cell-derived LCs, CD14<sup>+</sup> monocyte-derived DCs (moDCs) and LCs (moLCs), and CD1c<sup>+</sup> blood DCs-derived LCs (CD1c-LCs).**

CD34<sup>+</sup> cord blood HSCs were expanded for 3 days in serum-free X-vivo<sup>TM</sup>15 medium (Lonza, Switzerland) supplemented with: 50ng/ml SCF, FLT3-L, TPO each. *In vitro* LCs were generated as previously described (30). In brief, expanded CD34<sup>+</sup> cells (4x10<sup>4</sup>/ml) were cultured for 7 days in serum-free CellGenix® GMP DC medium (CellGenix, Germany) supplemented with: 100ng/ml GM-CSF, 50ng/ml FLT3-L, 20ng/ml SCF, 2.5ng/ml TNF $\alpha$ , and 1ng/ml TGF- $\beta$ 1 or 200ng/ml BMP7. For moDC generation, CD14<sup>+</sup> monocytes (1x10<sup>6</sup>/ml) were cultured for 6 days in RPMI-1640 + 10% FBS (Sigma-Aldrich, USA) supplemented with: 35ng/ml IL-4 and 100ng/ml GM-CSF. For CD1c-LC generation, peripheral blood CD1c<sup>+</sup>DCs (5x10<sup>5</sup>/ml) were cultured for 3-4 days in RPMI-1640 + 10% FBS supplemented with: 100ng/ml GM-CSF, and 10ng/ml TGF- $\beta$ 1 or 200ng/ml BMP7. For moLC generation, CD14<sup>+</sup> monocytes (1x10<sup>6</sup>/ml) were cultured for 5 days in Delta-1 coated plates (31) in RPMI-1640 + 10% FBS supplemented with: 100ng/ml GM-CSF, and 10ng/ml TGF- $\beta$ 1 or 200ng/ml BMP7.

**Flow cytometry**

Flow cytometry staining (extracellular epitopes) was performed as previously described (32). Data were acquired with LSRII instrument (BD Bioscience, USA) and analyzed with FlowJo software (Tree Star, Inc. USA). For the FACS sorting the BD FACS Aria flow cytometer (BD Bioscience, USA) was used. Monoclonal antibodies are listed in the supplementary table 1.

**Cytokine measurements**

Day 7 CD207<sup>+</sup>LCs were MACS sorted (purity  $\geq$ 90%) and activated with 5 $\mu$ g/ml PGN. After 48h supernatants were collected. The proteome profiler human cytokine array kit (R&D Systems, USA) was used according to the manufacturer's instructions. Spot intensity was quantified with ImageLab<sup>TM</sup> software (BioRad). For the quantitative measurement of cytokines in the supernatants from MLRs Luminex system was used.

170

**171 Dithranol clinical trial**

172 Paraffin-embedded materials from pre- and post-treatment (4 weeks after therapy completion) biopsy  
173 samples were available from six patients (5 men, 1 woman; age range 21-77 years) of a clinical study  
174 investigating the effect of topical dithranol in psoriasis. Dithranol study Clinical Trials.gov  
175 no.NCT02752672; approval number A23/15, Ethical Committee of the State of Carinthia, Austria.

**176 Statistics**

177 Statistical analysis was performed using 2-tailed *t*-test or one-way ANOVA (corrected with Tukey  
178 multiple comparison test) with GraphPad Prism6 software (GraphPad Software Inc.). p-values  $\leq 0.05$   
179 were considered significant.

180

181 Detailed description of cytokines and reagents, cell isolation, preparation of single cell suspension  
182 from psoriatic skin biopsies, RNA isolation and gene expression analysis, cytokine measurements,  
183 transmission electron microscopy, immunofluorescence and immunohistochemistry, mice, intradermal  
184 noggin injections in mice, dorsomorphin treatment, murine skin thickness measurement, and T-cell  
185 proliferation assay can be found in the supplemental material.

186

187

188

189

190

191

192

193

194



**Results*****BMP7-LCs are responsive to TLR2 stimulation***

We recently found that BMP7 replaces TGF- $\beta$ 1 in instructing LC differentiation from CD34<sup>+</sup> hematopoietic progenitor cells (24). Adding either TGF- $\beta$ 1 or BMP7 to a mix of cytokines in serum-free medium promotes the formation of E-cadherin-mediated clustering CD1a<sup>+</sup>CD207<sup>+</sup> LCs (Fig. 1A). TGF- $\beta$ 1- and BMP7-generated LCs (termed TGF- $\beta$ 1-LCs and BMP7-LCs, respectively) both exhibit phenotypic characteristics of LCs (CD1a<sup>+</sup>CD207<sup>+</sup>CD324<sup>+</sup> (24)). However, genome-wide microarray analyses of sorted CD1a<sup>+</sup>CD207<sup>+</sup> cells revealed several differentially expressed genes in BMP7-LCs vs. TGF- $\beta$ 1-LCs (Fig. 1B). Subsequent qRT-PCR analyses showed that both TGF- $\beta$ 1-LCs and BMP7-LCs lack detectable expression of several toll-like receptors (i.e. TLRs 3, 4, 5, 7, 8, 9), as also observed for *ex vivo* isolated LCs (33). However, BMP7-LCs express higher levels of bacterial recognition receptor TLR2 (Fig. 1C, 1D) and lower levels of TLR1, TLR6, as well as lower levels of anti-inflammatory TLR10 (34,35) than TGF- $\beta$ 1-LCs (Fig. 1C). Moreover, TLR2 positivity by BMP7-LCs is correlated with reduced CD207 expression (Fig. 1D). Bacterial ligand peptidoglycan (PGN) was added to TGF- $\beta$ 1-LCs vs. BMP7-LCs to analyze their cytokine/chemokine response to TLR2-mediated stimulation (Fig. 1E). Analyzing a limited panel of cytokines, we previously found that BMP7-LCs indeed exceed TGF- $\beta$ 1-LCs in PGN-induced cytokine production (24). We here confirmed and extended on these observations. BMP7-LCs responded to PGN with increased synthesis of several cytokines (i.e. TNF $\alpha$ , IL6, and GM-CSF) and chemokines (CXCL1, CCL3/4, and CCL1) relative to TGF- $\beta$ 1-LCs (Fig. 1E). Moreover, TGF- $\beta$ 1-LCs equaled BMP7-LCs in their basal and PGN-induced production of IL-8, IL-21, CCL2, ICAM1 and CCL5 (Fig. 1E). To further investigate functional aspects of BMP7-LCs, we performed a mixed lymphocyte reaction (MLR). This analysis showed that BMP7-LCs are not only more potent stimulators of T cell proliferation than TGF- $\beta$ 1-LCs (Fig. S1A), but they also primed naive CD4 T cells towards high production of GM-CSF, TNF $\alpha$ , IL-1 $\beta$ , and IL-2. Inversely, TGF- $\beta$ 1-LCs stimulated CD4 T cells to secrete high levels of anti-inflammatory IL-10 (Fig. S1B).

**223 *BMP7 promotes the generation of LCs exhibiting CD1c<sup>+</sup>CD206<sup>+</sup> phenotype***

224 Above-mentioned gene array profiling (Fig. 1B) revealed differential expression of several mRNAs  
225 encoding cell surface molecules. Subsequent flow cytometry showed that BMP7-LCs express higher  
226 levels of CD11c, CD1c, CD206, CD36, CD80, CXCR1 and CX3CR1, and lower levels of Trop2  
227 (TACSTD2) than TGF- $\beta$ 1-LCs (Fig. 2A). Therefore, BMP7-LCs differ from both *in vitro* generated  
228 TGF- $\beta$ 1-LCs and *ex vivo* isolated LCs in that they are CD1c<sup>hi</sup>CD206<sup>hi</sup>CD36<sup>hi</sup>TROP2<sup>lo/neg</sup>. Moreover,  
229 BMP7-LCs exhibit constitutively active canonical BMP signaling, as evidenced by their significantly  
230 higher expression level of pSmad1/5/8, when compared to TGF- $\beta$ 1-LCs (Fig. S2). Given their  
231 inflammation-associated characteristics (Fig.1, Fig. S1), we phenotypically compared BMP7-LCs to  
232 monocyte-derived DCs (moDCs) known to resemble inflammatory dendritic epidermal cells (IDECs)  
233 in eczema/atopic dermatitis lesions (36–39). BMP7-LCs clearly differed from moDCs in parallel  
234 analyses (compare Fig. S3 with Fig. 2A). First, moDCs lack LC-associated CD207, CD324/E-  
235 cadherin, EpCAM and TACSTD2/TROP2; Second, unlike BMP7-LCs, moDCs express high levels of  
236 CD209/DC-SIGN and CD11b (Fig. S3 (40,41)).

237

**238 *LCs generated from peripheral blood precursors are CD206<sup>+</sup>CD1c<sup>+</sup>***

239 Murine studies showed that during inflammation LCs develop from monocytes (10,11,13). Recently,  
240 human CD1c<sup>+</sup> blood DCs were identified as candidate LC precursors, since they rapidly (within 72h)  
241 differentiate into CD207<sup>+</sup>CD1a<sup>+</sup>LCs (19). Whether LCs generated from these cells phenotypically  
242 resemble inflammation-associated LCs remains unknown. We purified CD1c<sup>+</sup> blood DCs from MNCs  
243 by first depleting monocytes and B cells, followed by anti-CD1c positive selection. Importantly,  
244 CD1c<sup>+</sup> blood DCs were resolved as a distinct population from CD14<sup>+</sup> monocytes (Fig. 2B). Both  
245 CD1c<sup>+</sup> blood DCs and CD14<sup>+</sup> monocytes differentiated into CD206<sup>+</sup>CD1c<sup>+</sup>CD36<sup>+</sup>CD207<sup>+</sup>CD1a<sup>+</sup>LCs  
246 in both TGF- $\beta$ 1/GM-CSF and BMP7/GM-CSF cultures (Fig. 2C, 2D). Therefore, LCs generated from  
247 CD14<sup>+</sup> monocytes or CD1c<sup>+</sup> blood DCs exhibit a CD206<sup>+</sup>CD1c<sup>+</sup> phenotype, irrespective of whether  
248 they are generated in response to TGF- $\beta$ 1 or BMP7.

249

250

251 ***BMP7-LCs lack detectable Birbeck granules***

252 Birbeck granules (BG) represent a hallmark ultrastructural characteristic of LCs. It was previously  
253 shown that a subset of lesional psoriatic epidermal LCs lack detectable BG (37). Moreover, LC  
254 maturation has been associated with depletion of BG, due to reduction of the intracellular langerin  
255 pool (42). Duplicating previous findings (30,43), TGF- $\beta$ 1-LCs contained numerous intracytoplasmic  
256 BG. Conversely, BMP7-LCs lacked BG, despite positivity for CD207.

257

258 ***BMP7-LCs resemble psoriatic LCs and the psoriatic epidermis is marked by BMP7 induction***

259 CD207<sup>+</sup> cells from healthy skin are CD1c<sup>low/-</sup>CD206<sup>neg</sup>. Conversely, the psoriatic epidermis harbors  
260 CD207<sup>+</sup> cells with phenotypical resemblance to BMP7-LCs as they are also CD1c<sup>+</sup>CD206<sup>+</sup> (Fig. 3A,  
261 3B). Flow cytometry analysis of cells from lesional biopsies confirmed that CD207<sup>+</sup> cells found in  
262 psoriatic skin co-express CD1c, CD206 and TLR2, similar to BMP7-LCs (Fig. 3C). We also detected  
263 dermal CD206<sup>+</sup>CD1c<sup>+</sup> cells; however these cells lack CD207 (Fig. 3B). BMP receptors and  
264 downstream effectors can be analyzed *in situ*. BMPs bind to the type-II receptor (BMPRII), leading to  
265 the recruitment and phosphorylation of a BMP type-I receptor and downstream Smad1/5/8. Strikingly,  
266 CD207<sup>+</sup>LCs in healthy and psoriatic skin are marked by a strong BMPRII expression (Fig. 3D, 3E).  
267 As described previously by our group (24), BMP7 expression is confined to the basal/germinal  
268 keratinocyte layers, a predominant site of LC residency in healthy human skin (Fig. 4A). In marked  
269 contrast, BMP7 is expressed throughout the acanthotic epidermis, and LCs occur scattered in psoriatic  
270 lesions (Fig. 4B). Whereas the healthy epidermis exhibits a weak phospho-Smad1/5/8 staining pattern  
271 (Fig. 4C), psoriatic LCs and KCs show a strong nuclear accumulation of phospho-Smad1/5/8 (Fig.  
272 4D). JunB is a known psoriasis risk associated gene located on the PSOR6 locus, and JunB expression  
273 is downregulated in psoriatic lesional skin (44). Conversely c-Jun expression is enhanced in the basal  
274 layer potentially regulating keratinocyte proliferation (45). Tamoxifen (Tx)-induced, epidermal  
275 deletion of Jun/JunB in the *Jun<sup>ff</sup>JunB<sup>ff</sup>K5cre-ER<sup>T</sup>* mouse model causes a psoriasis-like disease (44),  
276 marked by strong lesional epidermal BMP7/phospho-Smad1/5/8 expression (Fig. 4E), duplicating  
277 findings in human. Thus, a genetic defect induced in adult KCs (i.e. Jun/JunB deletion) drives psoriatic  
278 lesion formation (44) associated with high BMP7 expression. Injection of the BMP antagonist noggin

279 (nog) is an established *in vivo* experimental approach to study the importance of BMP signaling in  
280 skin biology (46–49). Thus, we injected intradermally beads-adsorbed nog (nog) into the ears of  
281 *Jun<sup>ff</sup>JunB<sup>ff</sup>K5cre-ER<sup>T</sup>* mice 24 h prior to Jun/JunB deletion, and monitored ear swelling for 12  
282 consecutive days (Fig. 4F). Expectedly, as a result of noggin treatment we found diminished  
283 pSmad1/5/8 staining intensity in the epidermis (Fig. S4A). While control mice exhibited progressive  
284 ear thickening from days 5 onwards, nog injected mice showed significantly reduced ear swelling over  
285 the course of the experiment (Fig. 4G, 4H). Histological analysis confirmed decreased epidermal  
286 thickening in nog-injected compared to control-injected animals (Fig. 4I, 4J). Furthermore, treatment  
287 of developed lesions with topical application of the BMP pathway inhibitor dorsomorphin (targeting  
288 type 1 receptors Alk2, 3 and 6) resulted in decreased ear swelling in comparison to the control treated  
289 mice (Fig. S4B). In aggregate, these murine and human data demonstrate that the lesional psoriatic  
290 epidermis is characterized by aberrant high BMP7/phospho-Smad1/5/8 expression, and that BMP7-  
291 LCs phenotypically resemble lesional LCs (CD207<sup>+</sup>CD206<sup>+</sup>CD1c<sup>+</sup>).

292

### 293 ***BMP7 supplementation is associated with proliferation of CD207<sup>+</sup> LCs***

294 LC numbers gradually increase during skin development, and CD207<sup>+</sup>LCs undergo self  
295 -renewal *in vivo* (14). However, the epidermal factors promoting LC proliferation remain unknown.  
296 Interestingly, BMP7-supplemented cultures showed vigorous proliferation, increased total cellularity  
297 and elevated numbers of LCs, relative to TGF- $\beta$ 1-supplemented cultures (Fig. 5A, 5B); We detected  
298 mitotic Ki67<sup>+</sup> cells among CD207<sup>+</sup>LCs, with percentages Ki67<sup>+</sup> cells being much higher for BMP7-  
299 LC than for TGF- $\beta$ -LCs (Fig. 5C, 5D). Therefore, BMP7 signaling allows active cycling of *in vitro*  
300 generated LCs. In the healthy adult epidermis, BMP7 expression is confined to basal KCs (Fig. 4A;  
301 5E, left; (24)). We analysed whether Ki67<sup>+</sup>LCs, known to occur in the healthy epidermis (14), co-  
302 localize with BMP7<sup>+</sup>KCs *in situ*. Indeed, Ki67<sup>+</sup>LCs and Ki67<sup>+</sup>KCs are confined to the BMP7<sup>+</sup>  
303 epidermal layers (Fig. 5E, left, 5G). In comparison, higher numbers of Ki67<sup>+</sup>CD207<sup>+</sup>LCs and  
304 Ki67<sup>+</sup>KC are observed in the lesional BMP7<sup>hi</sup> psoriatic epidermis (Fig. 5E right, 5F). In inflamed skin  
305 the confinement of proliferating cells to the basal epidermal layer was lost, and proliferating LCs and  
306 KCs could be found throughout the enlarged BMP7<sup>hi</sup> epidermis (Fig. 5E, right; model in Fig. S5).

307 **Canonical TGF- $\beta$ 1-ALK5 signaling inhibits phenotypic characteristics of BMP7-LCs**

308 In healthy human epidermis, TGF- $\beta$ 1 is expressed in supra-basal/outer KC layers; conversely, BMP7  
309 is confined to basal KCs (Fig. 4A; 5E (24)). Canonical TGF- $\beta$ 1-ALK5 signaling is required to retain  
310 LCs in a non-activated state *in situ* (27). TGF- $\beta$ 1 co-activates both ALK5 and ALK3 (Fig. 6A), the  
311 latter being required for TGF- $\beta$ 1-dependent LC differentiation *in vitro* (24); conversely, BMP7 signals  
312 through ALK3 but not ALK5 (Fig. 6A; (24,50,51)). BMP7-LCs and lesional psoriatic LCs are  
313 CD1c<sup>+</sup>/CD206<sup>+</sup>, whereas TGF- $\beta$ 1-LCs and steady-state LCs lack these markers (Fig. 2A, 3A). We  
314 therefore investigated whether active ALK5 signaling represses CD1c and CD206. Indeed, short-term  
315 (48 h) stimulation of BMP7-LCs with TGF- $\beta$ 1 downregulated both CD1c and CD206 (Fig. 6B, lower  
316 panel). We performed an inversed experiment to validate these findings. Pharmacological inhibition of  
317 the ALK5 receptor in TGF- $\beta$ 1-LC cultures dose-dependently led to the re-establishment of the  
318 CD1c<sup>+</sup>CD206<sup>+</sup> LC phenotype (Fig. 6C). Together these data revealed that selective ALK3 activation  
319 by BMP7 induces a CD1c<sup>+</sup>CD206<sup>+</sup> LC phenotype, whereas co-activation of the canonical TGF- $\beta$ 1-  
320 ALK5 cascade represses CD1c and CD206.

321

322 **Topical treatment of psoriatic lesions diminishes BMP7 expression**

323 Topical treatment of psoriatic lesions with dithranol (anthralin) inhibits KC proliferation (52), and our  
324 murine data indicate a KC-intrinsic mechanism of BMP7 induction during the onset of psoriatic-like  
325 epidermal hyperplasia (Fig. 4E). We monitored BMP7 expression in serial lesional skin biopsies  
326 before and after dithranol treatment of psoriatic patients (n=6). Expectedly, before treatment BMP7  
327 was expressed throughout the lesional epidermis (Fig 7A). Four weeks after treatment initiation,  
328 BMP7 staining intensity was markedly reduced with only basal KC layers staining positive for BMP7  
329 (Fig. 7A), similarly as observed in the healthy skin (Fig. 4A). The clinical status of the patients was  
330 monitored using the psoriasis area and severity index (PASI) score. Out of six analysed patients, after  
331 treatment, four exhibited a substantial reduction in BMP7 staining intensity. (Fig. 7A, diagram).  
332 Correlation analysis revealed a positive correlation between BMP7 reduction and PASI score  
333 reduction (Fig. 7B). All four patients with strong BMP7 reduction also had strong reduction in PASI

334 score. Conversely, the patient who had no BMP7 decrease also had no PASI score improvement after  
335 the completion of the therapy (Fig. 7B).

336

337

338

339

340

341

342

343

344

345

346

347

348

349

350

351

352

353

354

355

356

357

358

359

360

361

362

Journal Pre-proof

**Discussion**

363  
364 Cutaneous psoriatic lesions are characterized by epidermal hyperplasia and are populated by  
365 bone marrow-derived epidermal LC-like cells (6,53). However, the epidermal factors instructing LC  
366 differentiation under normal and diseased conditions are poorly defined. While we previously showed  
367 that BMP7 is confined to the basal KC layer in the healthy epidermis (24), we here demonstrated that  
368 BMP7 and associated downstream BMP signaling components (i.e. phospho-SMAD1/5/8) are highly  
369 expressed throughout the enlarged psoriatic epidermis. Using gene profiling, we further showed that  
370 BMP7 induces the generation of CD1c<sup>+</sup>CD206<sup>+</sup>LCs *in vitro*, phenotypically mimicking psoriasis-  
371 associated LC-like cells. Moreover, a substantial fraction of *in vitro* generated BMP7-LCs exhibited  
372 mitotic activity, similarly as observed for psoriatic LCs *in situ*. We previously showed that ~40% of  
373 CD207<sup>+</sup>LCs in murine psoriatic lesions are of bone marrow origin, and these cells exceeded host-  
374 derived LCs in mitotic activity (7). Extending on these analyses we here showed that induction of  
375 psoriatic lesions by genetic targeting of adult KCs in Jun<sup>fl/fl</sup>JunB<sup>fl/fl</sup> K5cre-ER<sup>T</sup> mice also causes a  
376 BMP7<sup>hi</sup>/phospho-SMAD1/5/8<sup>hi</sup> phenotype, indicating a KC-intrinsic mechanism for BMP7 induction.  
377 Together these data suggest a key role for epidermal KC-derived BMP7 in instructing LC  
378 differentiation from bone marrow-derived precursors in psoriatic lesions (see hypothetical model in  
379 Fig. S5). Furthermore, we demonstrated that lesional BMP7 is strongly diminished upon dithranol  
380 treatment of psoriatic patients, and that epidermal BMP7 reduction correlates with clinical  
381 improvement. Moreover, injection of BMP antagonist noggin in Jun<sup>fl/fl</sup>JunB<sup>fl/fl</sup> K5cre-ER<sup>T</sup> mice led to  
382 the reduction in epidermal thickening, indicating involvement of BMP signaling in psoriatic lesion  
383 formation.

384 Our phospho-Smad1/5/8 stainings support that the BMP pathway is aberrantly activated in the  
385 psoriatic epidermis. However, despite high expression of BMP7 protein throughout the lesional KCs,  
386 BMP7 might not be the only BMP family member expressed in the psoriatic epidermis. Interestingly,  
387 psoriatic epidermal lesions were previously shown to exhibit diminished canonical TGF- $\beta$  signaling,  
388 as evidenced by decreased levels of TGF- $\beta$  type-I receptor ALK5, TGF- $\beta$ R type-II and phospho-  
389 SMAD2/3 (54,55). Moreover, TGF- $\beta$ 2 and TGF- $\beta$ 3 (54,56) are downregulated and inhibitory SMAD7  
390 is induced in the psoriatic epidermis (57). We here showed that the inhibition of ALK5 signaling

391 (canonical TGF- $\beta$ 1 signaling) in TGF- $\beta$ 1-LC cultures results in the generation of CD1c<sup>hi</sup>CD206<sup>hi</sup> LCs  
392 (mimicking lesional LCs). Inversely, adding TGF- $\beta$ 1 to BMP7-LC cultures led to the repression of  
393 CD1c and CD206. In line with impairment of canonical TGF- $\beta$ 1 signaling in inflammation, Bobr et.  
394 al. demonstrated that a portion of murine LCs stain positive for phospho-SMAD2/3 (downstream of  
395 TGF- $\beta$ 1-ALK5) in normal but not in inflamed skin (27).

396 A side-by-side comparison revealed that BMP7-supplemented LC cultures give rise to much  
397 higher numbers of human LCs compared to TGF- $\beta$ 1-supplemented cultures. Our data suggest a  
398 sequential protocol for the generation of high numbers of LCs from human progenitor cells (i.e. BMP7  
399 followed by TGF- $\beta$ 1) in defined serum-free media for cell therapy-oriented studies. We showed that  
400 high percentages of *in vitro* generated CD207<sup>+</sup>BMP7-LCs are Ki67<sup>+</sup>, indicating that BMP7-ALK3  
401 signaling facilitates LC cycling. In line with this, the type-II BMP receptor BMPR2 is strongly  
402 expressed by LCs *in situ*, and marks LCs in epidermal immunohistology. Consistent with a role of  
403 BMP7 in facilitating LC cycling, we observed that Ki67<sup>+</sup>LCs, known to reside in the healthy  
404 epidermis (14,58), are confined to the BMP7<sup>+</sup>KC layers. Moreover, Ki-67<sup>+</sup>LCs occurred abundantly  
405 and spatially scattered throughout the BMP7<sup>hi</sup> human psoriatic epidermis. Since lesional psoriatic LCs  
406 undergo physical clustering with T cells (9), BMP7 might be critically involved in this process.

407 During ontogeny LC precursors within the epidermal niche are first exposed to BMP7  
408 followed by TGF- $\beta$ 1 (24,59). TGF- $\beta$ 1-ALK5 signaling enables LCs to remain in their non-activated  
409 state, a model directly supported by murine ALK5 (29) and TGF- $\beta$ R2 (26) knock-out studies.  
410 Moreover, sequential BMP7/TGF- $\beta$ 1 signaling was shown to instruct murine mucosal LCs  
411 differentiation (60); reviewed in: (61). Notably, supernatants of cultured keratinocytes (pre-stimulated  
412 or not with IL-17 and TNF $\alpha$ ) failed to replace exogenous BMP7 for the promotion of LC  
413 differentiation from CD34<sup>+</sup> cells (unpublished observation). Therefore, cell contact-dependent  
414 mechanisms might be required for these effects, e.g. enabling BMP7 processing.

415 Freshly isolated human LCs were shown to lack detectable TLR4 and to express low or  
416 undetectable TLR5 and TLR2 (46,62,63). Van der Aar et al. (63) previously showed that these  
417 bacterial recognition receptors are repressed upon TGF- $\beta$ 1 stimulation of monocytes undergoing  
418 moLC differentiation and that dermal DCs express these TLRs. Consistently, we here showed that  
419 TGF- $\beta$ 1-LCs lack detectable TLR4, TLR5 and TLR2. Moreover, *in vitro* generated CD34<sup>+</sup> cell-



420 derived LCs in our study resembled *ex vivo* isolated LCs in detectable expression of TLR1, TLR6  
421 (33,63) and TLR10 (33), as well as in low/non-detectable TLR7 and TLR8 (33). However,  
422 inconsistent data have been published regarding the expression of TLR7/9/10 by *ex vivo* isolated LCs  
423 (33,62,63). Notably, while TLR3 is expressed by LCs and moLCs (63), we failed to detect TLR3 in  
424 CD34<sup>+</sup> cell-derived LCs. Whether these differences are inherent to the specific culture models studied  
425 remains to be analyzed. We showed here using flow cytometry that BMP7-LCs are TLR2<sup>+</sup>, whereas  
426 TGF- $\beta$ 1-LCs lack detectable TLR2. Moreover, TGF- $\beta$ 1-LCs exceeded BMP7-LCs in levels of  
427 TLR10mRNA expression. Interestingly, TLR10 is regarded as the only known inhibitory receptor  
428 within the TLR family (recently reviewed in: (64)). TLR10 is able to homodimerize and  
429 heterodimerize with TLR1 and TLR2. Elevated TLR2 and diminished TLR10, observed in BMP7-LCs  
430 relative to TGF- $\beta$ 1-LCs, might thus contribute to the here observed more potent cytokine production  
431 of the former in response to PGN stimulation. It will be interesting to further analyze whether TLR10  
432 is expressed by *in vivo* LCs and if so, whether lesional psoriatic LCs exhibit diminished levels of  
433 TLR10. It is interesting to speculate that an inverse expression of TLR2/TLR10 might sensitize LCs  
434 from lesional psoriatic skin to gram positive bacteria such as *Staphylococcus aureus*. In line with this  
435 possibility, we detected substantial levels of TLR2 on LCs from lesional psoriatic skin. Consistently,  
436 PGN-stimulated BMP7-LCs produced higher levels of several inflammatory mediators (e.g.: IL6,  
437 TNF $\alpha$ , CXCL1, CCL3/4) relative to TGF- $\beta$ 1-LCs. Our observations are consistent with the  
438 demonstration that TLR2 stimulated LCs are potent inducers of Th17 polarization, highlighting the  
439 importance of TLR2 in immune responses in inflamed skin (65). Future studies are required to analyze  
440 *in vitro* generated LCs for additional cytokines such as IL-22 and IL-23 known to be involved in  
441 psoriasis. Moreover, intracellular cytokine staining needs to be performed to determine the cellular  
442 origin of the cytokines measured in the supernatants of LC-T cells co-cultures.

443 CD207<sup>+</sup> BMP7-LCs phenotypically resemble LCs found in lesional psoriatic skin in that these  
444 cells are also CD1c<sup>+</sup>CD206<sup>+</sup>. Similarly, LCs generated *in vitro* from monocytes or from peripheral  
445 blood CD1c<sup>+</sup> DCs express CD1c and CD206, consistent with the concept that these cells may develop  
446 into LCs during inflammation (reviewed in: (66)). A monocyte origination of LCs is also evident from  
447 studies on their development from CD34<sup>+</sup> cells *in vitro*. Monocyte intermediates which arise in these  
448 cultures have to lose expression of the monocyte identity factor KLF4, in order to differentiate into

449 LCs (67). In conclusion, our data are consistent with a model whereby monocytes immigrate to the  
450 psoriatic epidermis and there differentiate into CD207<sup>+</sup>CD1a<sup>+</sup>CD1c<sup>+</sup>CD206<sup>+</sup> LCs. It has been  
451 previously shown that in psoriasis CD206 is expressed by a subset of CD1a<sup>+</sup> epidermal cells (37).  
452 Whether human inflammation-associated CD207<sup>+</sup>CD1c<sup>+</sup>CD206<sup>+</sup> LC arise from myeloid progenitor  
453 cells, CD14<sup>+</sup> monocytes or CD1c<sup>+</sup> blood DC remains to be studied. In this context it is interesting to  
454 note that BMP7-LCs phenotypically differed from moDCs, previously shown to resemble atopic  
455 dermatitis-associated IDECs (36–39).

456 Our results demonstrated, that *in vitro* BMP7-LCs express higher levels of several pro-  
457 inflammatory genes and exhibit more potent T cell stimulatory capacity than TGF-β1-LCs. This is  
458 consistent with the observation that CD1a on LCs facilitates psoriatic skin inflammation both in  
459 patients and the murine system (68). However, a regulatory function of these cells *in vivo* cannot be  
460 ruled out, considering previously demonstrated regulatory properties of semi-mature or even mature  
461 DCs (69); recently reviewed in: (70). With regards to a possible function of psoriatic inflammation-  
462 associated LCs, we previously showed that LCs are dispensable for the induction phase of psoriatic  
463 lesions in Jun<sup>f/f</sup>JunB<sup>f/f</sup> K5cre-ER<sup>T</sup> mice; however they exerted an immune-regulatory function in  
464 chronic lesions (7). Despite our here presented observations that murine lesions in these mice are also  
465 BMP7<sup>hi</sup>/p-SMAD1/5/8<sup>hi</sup>, a direct translation of these findings to the human system must take into  
466 account major species differences; recently reviewed in: (70).

467 We showed that TGF-β1 stimulation represses CD1c and CD206 expression in LCs generated  
468 in response to BMP7. It will be interesting to perform therapy-oriented *in vivo* studies addressing  
469 whether bone marrow-derived psoriatic LCs might differentiate further into steady-state-like LCs  
470 during the resolution phase of cutaneous psoriatic lesions, and whether this process is driven or can be  
471 augmented by TGF-β-ALK5 signaling. Moreover, future studies are required to address the molecular  
472 mechanism of enhanced BMP7 expression in psoriatic lesions. Among several factors, high BMP7  
473 levels throughout the epidermal psoriatic lesions might be due to the expansion of basal keratinocytes  
474 or enhanced processing of BMP7 precursor molecules.

475 In conclusion, our data indicate that available TGF-β family members within psoriatic  
476 epidermal lesions preferentially activate the BMP signaling cascade, leading to the generation of

477 proliferative, inflammation-associated LCs. Therapeutically targeting of this pathway, or restoration of  
478 canonical TGF- $\beta$  signaling, might allow for interfering with cutaneous psoriatic lesion formation.

479 .

480

481

482

483

484

485

486

487

488

489

490

491

492

493

494

495

496

497

498

499

Journal Pre-proof

**Acknowledgments**

501 We thank E. Schwarzenberger for cell preparation and technical assistance, T. Brossmann for PCR  
502 mice genotyping and sample embedding, I. Fedorenko for technical assistance in EM-sample  
503 preparation, and T. Bauer for designing the graphical abstract.

504

505

506

507

508

509

510

511

512

513

514

515

516

517

518

519

520

521

522

523

524

525

526

527

528 **References**

529

- 530 1. Heath WR, Carbone FR. The skin-resident and migratory immune system in steady state and  
531 memory: Innate lymphocytes, dendritic cells and T cells. *Nat Immunol.* 2013;14(10):978–85.
- 532 2. Hatakeyama M, Fukunaga A, Washio K, Taguchi K, Oda Y, Ogura K, et al. Anti-Inflammatory  
533 Role of Langerhans Cells and Apoptotic Keratinocytes in Ultraviolet-B–Induced Cutaneous  
534 Inflammation. *J Immunol.* 2017;199(8):2937–47.
- 535 3. Seneschal J, Clark RA, Gehad A, Baecher-Allan CM, Kupper TS. Human Epidermal  
536 Langerhans Cells Maintain Immune Homeostasis in Skin by Activating Skin Resident  
537 Regulatory T Cells. *Immunity.* 2012;36(5):873–84.
- 538 4. Kitashima DY, Kobayashi T, Woodring T, Idouchi K, Doebel T, Voisin B, et al. Langerhans  
539 Cells Prevent Autoimmunity via Expansion of Keratinocyte Antigen-Specific Regulatory T  
540 Cells. *EBioMedicine.* 2018;27:293–303.
- 541 5. Lowes MA, Suarez-Farinas M, Krueger JG. Immunology of Psoriasis. *Annu Rev Immunol.*  
542 2014;32:227–55.
- 543 6. Martini E, Wikén M, Cheuk S, Gallais Sérézal I, Baharom F, Stähle M, et al. Dynamic  
544 Changes in Resident and Infiltrating Epidermal Dendritic Cells in Active and Resolved  
545 Psoriasis. *J Invest Dermatol.* 2017;137(4):865–73.
- 546 7. Glitzner E, Korosec A, Brunner PM, Drobits B, Amberg N, Schonthaler HB, et al. Specific  
547 roles for dendritic cell subsets during initiation and progression of psoriasis. *EMBO Mol Med.*  
548 2014;6(10):1312–27.
- 549 8. Terhorst D, Chelbi R, Wohn C, Malosse C, Tamoutounour S, Jorquera A, et al. Dynamics and  
550 Transcriptomics of Skin Dendritic Cells and Macrophages in an Imiquimod-Induced, Biphasic  
551 Mouse Model of Psoriasis. *J Immunol.* 2015;195(10):4953–61.
- 552 9. Eidsmo L, Martini E. Human Langerhans cells with pro-inflammatory features relocate within  
553 psoriasis lesions. *Front Immunol.* 2018;9(FEB):1–8.
- 554 10. Ginhoux F, Tacke F, Angeli V, Bogunovic M, Loubreau M, Dai XM, et al. Langerhans cells  
555 arise from monocytes in vivo. *Nat Immunol.* 2006;7(3):265–73.
- 556 11. Sere K, Baek JH, Ober-Blobaum J, Muller-Newen G, Tacke F, Yokota Y, et al. Two Distinct

- 557 Types of Langerhans Cells Populate the Skin during Steady State and Inflammation. *Immunity*.  
558 2012;37(5):905–16.
- 559 12. Chopin M, Seillet C, Chevrier S, Wu L, Wang H, Morse 3rd HC, et al. Langerhans cells are  
560 generated by two distinct PU.1-dependent transcriptional networks. *J Exp Med*.  
561 2013;210(13):2967–80.
- 562 13. Singh TP, Zhang HH, Borek I, Wolf P, Hedrick MN, Singh SP, et al. Monocyte-derived  
563 inflammatory Langerhans cells and dermal dendritic cells mediate psoriasis-like inflammation.  
564 *Nat Commun*. 2016;7(May):1–18.
- 565 14. Chorro L, Sarde A, Li M, Woollard KJ, Chambon P, Malissen B, et al. Langerhans cell (LC)  
566 proliferation mediates neonatal development, homeostasis, and inflammation-associated  
567 expansion of the epidermal LC network. *J Exp Med*. 2009;206(13):3089–100.
- 568 15. Mende I, Karsunky H, Weissman IL, Engleman EG, Merad M. Flk2+ myeloid progenitors are  
569 the main source of Langerhans cells. *Blood*. 2006;107(4):1383–90.
- 570 16. Schuster C, Mildner M, Mairhofer M, Bauer W, Fiala C, Prior M, et al. Human embryonic  
571 epidermis contains a diverse Langerhans cell precursor pool. *Development*. 2014;141(4):807–  
572 15.
- 573 17. Capucha T, Mizraji G, Segev H, Blecher-Gonen R, Winter D, Khalaileh A, et al. Distinct  
574 Murine Mucosal Langerhans Cell Subsets Develop from Pre-dendritic Cells and Monocytes.  
575 *Immunity*. 2015;43(2):369–81.
- 576 18. Martínez-Cingolani C, Grandclaoudon M, Jeanmougin M, Jouve M, Zollinger R, Soumelis V.  
577 Human blood BDCA-1 dendritic cells differentiate into Langerhans-like cells with thymic  
578 stromal lymphopoietin and TGF- $\beta$ . *Blood*. 2014;124(15):2411–20.
- 579 19. Milne P, Bigley V, Gunawan M, Haniffa M, Collin M. CD1c<sup>+</sup> blood dendritic cells have  
580 Langerhans cell potential. *Blood*. 2015;125(3):470–4.
- 581 20. Larregina AT, Morelli AE, Spencer LA, Logar AJ, Watkins SC, Thomson AW, et al. Dermal-  
582 resident CD14<sup>+</sup> cells differentiate into Langerhans cells. *Nat Immunol*. 2001;2(12):1151–8.
- 583 21. Hoshino N, Katayama N, Shibasaki T, Ohishi K, Nishioka J, Masuya M, et al. A novel role for  
584 Notch ligand Delta-1 as a regulator of human Langerhans cell development from blood  
585 monocytes. *J Leukoc Biol*. 2005;78(4):921–9.

- 586 22. Jurkin J, Krump C, Köffel R, Fieber C, Schuster C, Brunner PM, et al. Human skin dendritic  
587 cell fate is differentially regulated by the monocyte identity factor Kruppel-like factor 4 during  
588 steady state and inflammation. *J Allergy Clin Immunol.* 2017;139(6).
- 589 23. Strobl H, Krump C, Borek I. Micro-environmental signals directing human epidermal  
590 Langerhans cell differentiation. *Semin Cell Dev Biol.* 2018;S1084-9521(17):30350–6.
- 591 24. Yasmin N, Bauer T, Modak M, Wagner K, Schuster C, Köffel R, et al. Identification of bone  
592 morphogenetic protein 7 (BMP7) as an instructive factor for human epidermal Langerhans cell  
593 differentiation. *J Exp Med.* 2013;210(12):2597–610.
- 594 25. Borkowski TA, Letterio JJ, Farr AG, Udey MC. A role for endogenous transforming growth  
595 factor beta 1 in Langerhans cell biology: the skin of transforming growth factor beta 1 null  
596 mice is devoid of epidermal Langerhans cells. *J Exp Med.* 1996;184(6):2417–22.
- 597 26. Kaplan DH, Li MO, Jenison MC, Shlomchik WD, Flavell RA, Shlomchik MJ.  
598 Autocrine/paracrine TGFbeta1 is required for the development of epidermal Langerhans cells. *J*  
599 *Exp Med.* 2007;204(11):2545–52.
- 600 27. Bobr A, Igyarto BZ, Haley KM, Li MO, Flavell RA, Kaplan DH. Autocrine / paracrine TGF-  $\beta$   
601 1 inhibits Langerhans cell migration. *Proc Natl Acad Sci U S A.* 2012;109(26):10492–7.
- 602 28. Kel JM, Girard-Madoux MJH, Reizis B, Clausen BE. TGF- Is Required To Maintain the Pool  
603 of Immature Langerhans Cells in the Epidermis. *J Immunol.* 2010;185(6):3248–55.
- 604 29. Zahner SP, Kel JM, Martina CAE, Brouwers-Haspels I, van Roon MA, Clausen BE.  
605 Conditional Deletion of TGF- $\beta$ R1 Using Langerin-Cre Mice Results in Langerhans Cell  
606 Deficiency and Reduced Contact Hypersensitivity. *J Immunol.* 2011;187(10):5069–76.
- 607 30. Strobl H, Riedl E, Scheinecker C, Bello-Fernandez C, Pickl WF, Rappersberger K, et al. TGF-  
608 beta 1 promotes in vitro development of dendritic cells from CD34+ hemopoietic progenitors. *J*  
609 *Immunol.* 1996;157(4):1499–507.
- 610 31. Varnum-Finney B, Wu L, Yu M, Brashem-Stein C, Staats S, Flowers D, et al. Immobilization  
611 of Notch ligand, Delta-1, is required for induction of notch signaling. *J Cell Sci.* 2000;113 Pt  
612 23:4313–8.
- 613 32. Platzer B, Jörgl A, Taschner S, Höcher B, Strobl H, Platzer B, et al. RelB regulates human  
614 dendritic cell subset development by promoting monocyte intermediates. *Blood.*

- 615 2014;104(12):3655–63.
- 616 33. Flacher V, Bouschbacher M, Verronese E, Massacrier C, Sisirak V, Berthier-Vergnes O, et al.  
617 Human Langerhans Cells Express a Specific TLR Profile and Differentially Respond to  
618 Viruses and Gram-Positive Bacteria. *J Immunol.* 2006;177(11):7959–67.
- 619 34. Oosting M, Cheng S-C, Bolscher JM, Vestering-Stenger R, Plantinga TS, Verschueren IC, et  
620 al. Human TLR10 is an anti-inflammatory pattern-recognition receptor. *Proc Natl Acad Sci.*  
621 2014;111(42):E4478–84.
- 622 35. Jiang S, Li X, Hess NJ, Guan Y, Tapping RI. TLR10 Is a Negative Regulator of Both MyD88-  
623 Dependent and -Independent TLR Signaling. *J Immunol.* 2016;196(9):3834–41.
- 624 36. Wollenberg A, Kraft S, Hanau D, Bieber T. Immunomorphological and ultrastructural  
625 characterization of Langerhans cells and a novel, inflammatory dendritic epidermal cell (IDEC)  
626 population in lesional skin of atopic eczema. *J Invest Dermatol.* 1996;106(3):446–53.
- 627 37. Wollenberg A, Mommaas M, Opiel T, Schottdorf E-M, Günther S, Moderer M. Expression  
628 and function of the mannose receptor CD206 on epidermal dendritic cells in inflammatory skin  
629 diseases. *J Invest Dermatol.* 2002;118:327–34.
- 630 38. Novak N, Kraft S, Haberstok J, Geiger E, Allam P, Bieber T. A reducing microenvironment  
631 leads to the generation of FcεRIhighinflammatory dendritic epidermal cells (IDEC). *J Invest*  
632 *Dermatol.* 2002;119(4):842–9.
- 633 39. Dijkstra D, Stark H, Chazot PL, Shenton FC, Leurs R, Werfel T, et al. Human Inflammatory  
634 Dendritic Epidermal Cells Express a Functional Histamine H4 Receptor. *J Invest Dermatol.*  
635 2008;128:1696–703.
- 636 40. Relloso M, Puig-Kroger A, Pello OM, Rodriguez-Fernandez JL, de la Rosa G, Longo N, et al.  
637 DC-SIGN (CD209) Expression Is IL-4 Dependent and Is Negatively Regulated by IFN, TGF-,  
638 and Anti-Inflammatory Agents. *J Immunol.* 2002;168(6):2634–43.
- 639 41. Plantinga M, Guilliams M, Vanheerswynghels M, Deswarte K, Branco-Madeira F, Toussaint  
640 W, et al. Conventional and Monocyte-Derived CD11b+Dendritic Cells Initiate and Maintain T  
641 Helper 2 Cell-Mediated Immunity to House Dust Mite Allergen. *Immunity.* 2013;38(2):322–  
642 35.
- 643 42. Mc Dermott R, Ziyilan U, Spehner D, Bausinger H, Lipsker D, Mommaas M, et al. Birbeck



- 644 granules are subdomains of endosomal recycling compartment in human epidermal langerhans  
645 cells, which form where langerin accumulates. *Mol Biol Cell*. 2002;13:317–35.
- 646 43. Caux C, Massacrier C, Dubois B, Valladeau J, Dezutter-Dambuyant C, Durand I, et al.  
647 Respective involvement of TGF- $\beta$  and IL-4 in the development of Langerhans cells and non-  
648 Langerhans dendritic cells from CD34+progenitors. *J Leukoc Biol*. 1999;66(5):781–91.
- 649 44. Zenz R, Eferl R, Kenner L, Florin L, Hummerich L, Mehic D, et al. Psoriasis-like skin disease  
650 and arthritis caused by inducible epidermal deletion of Jun proteins. *Nature*.  
651 2005;437(7057):369–75.
- 652 45. Mehic D, Bakiri L, Ghannadan M, Wagner EF, Tschachler E. Fos and Jun proteins are  
653 specifically expressed during differentiation of human keratinocytes. *J Invest Dermatol*.  
654 2005;124(1):212–20.
- 655 46. Plikus M V, Mayer J, Cruz D De, Baker RE, Maini PK, Maxson R, et al. Cyclic dermal BMP  
656 signaling regulates stem cell activation during hair regeneration. *Nature*. 2008;451(7176):340–  
657 4.
- 658 47. Greco V, Chen T, Rendl M, Schober M, Pasolli HA, Stokes N, et al. A Two-Step Mechanism  
659 for Stem Cell Activation during Hair Regeneration. *Cell*. 2009;4(2):155–69.
- 660 48. Oshimori N, Fuchs E. Paracrin TGF-beta signaling Counterbalance BMP-mediated Repression  
661 in Hair Follicle Stem Cell Activation. *Cell Stem Cell*. 2012;10(1):63–75.
- 662 49. Lee J, Kang S, Lilja KC, Colletier KJ, Scheitz CJF, Zhang Y V, et al. Signalling couples hair  
663 follicle stem cell quiescence with reduced histone H3 K4/K9/K27me3 for proper tissue  
664 homeostasis. *Nat Commun*. 2016;7:11278.
- 665 50. Daly AC, Randall RA, Hill CS. Transforming Growth Factor beta-Induced Smad1/5  
666 Phosphorylation in Epithelial Cells Is Mediated by Novel Receptor Complexes and Is Essential  
667 for Anchorage-Independent Growth. *Mol Cell Biol*. 2008;28(22):6889–902.
- 668 51. Miyazono K, Kamiya Y, Morikawa M. Bone morphogenetic protein receptor and signal  
669 transduction. *J Biochem*. 2010;147(1):35–51.
- 670 52. Holstein J, Fehrenbacher B, Brück J, Müller-Hermelink E, Schäfer I, Carevic M, et al.  
671 Anthralin modulates the expression pattern of cytokeratins and antimicrobial peptides by  
672 psoriatic keratinocytes. *J Dermatol Sci*. 2017;87(3):236–45.

- 673 53. Korenfeld D, Gorvel L, Munk A, Man J, Schaffer A, Tung T, et al. A type of human skin  
674 dendritic cell marked by CD5 is associated with the development of inflammatory skin disease.  
675 J Clin Invest. 2017;2(18):e96101.
- 676 54. Doi H, Shibata MA, Kiyokane K, Otsuki Y. Downregulation of TGF $\beta$  isoforms and their  
677 receptors contributes to keratinocyte hyperproliferation in psoriasis vulgaris. J Dermatol Sci.  
678 2003;33(1):7–16.
- 679 55. Jiang M, Sun Z, Dang E, Li B, Fang H, Li J, et al. TGF $\beta$ /SMAD/microRNA-486-3p Signaling  
680 Axis Mediates Keratin 17 Expression and Keratinocyte Hyperproliferation in Psoriasis. J Invest  
681 Dermatol. 2017;137(10):2177–86.
- 682 56. Wataya-Kaneda M, Hashimoto K, Kato M, Miyazono K, Yoshikawa K. Differential  
683 localization of TGF-beta-precursor isoforms in psoriatic human skin. J Dermatol Sci.  
684 1996;11(3):183–8.
- 685 57. Di Fusco D, Laudisi F, Dinallo V, Monteleone I, Di Grazia A, Marafini I, et al. Smad7  
686 positively regulates keratinocyte proliferation in psoriasis. Br J Dermatol. 2017;177(6):1633–  
687 43.
- 688 58. Kanitakis J, Morelon E, Petruzzo P, Badet L, Dubernard JM. Self-renewal capacity of human  
689 epidermal Langerhans cells: Observations made on a composite tissue allograft. Exp Dermatol.  
690 2011;20(2):145–6.
- 691 59. Schuster C, Vaculik C, Fiala C, Meindl S, Brandt O, Imhof M, et al. HLA-DR+ leukocytes  
692 acquire CD1 antigens in embryonic and fetal human skin and contain functional antigen-  
693 presenting cells. J Exp Med. 2009;206(1):169–81.
- 694 60. Capucha T, Koren N, Nassar M, Heyman O, Nir T, Levy M, et al. Sequential BMP7/TGF- $\beta$ 1  
695 signaling and microbiota instruct mucosal Langerhans cell differentiation. J Exp Med.  
696 2018;215(2):481–500.
- 697 61. Hovav AH. Mucosal and Skin Langerhans Cells – Nurture Calls. Trends Immunol.  
698 2018;39(10):788–800.
- 699 62. Peiser M, Koeck J, Kirschning CJ, Wittig B, Wanner R. Human Langerhans cells selectively  
700 activated via Toll-like receptor 2 agonists acquire migratory and CD4 + T cell stimulatory  
701 capacity . J Leukoc Biol. 2008;83(5):1118–27.

- 702 63. van der Aar AMG, Sylva-Steenland RMR, Bos JD, Kapsenberg ML, de Jong EC, Teunissen  
703 MBM. Cutting Edge: Loss of TLR2, TLR4, and TLR5 on Langerhans Cells Abolishes  
704 Bacterial Recognition. *J Immunol.* 2007;178(4):1986–90.
- 705 64. Nagashima H, Yamaoka Y. Importance of toll-like receptors in pro-inflammatory and anti-  
706 inflammatory responses by helicobacter pylori infection. *Curr Top Microbiol Immunol.*  
707 2019;421:139–58.
- 708 65. Aliahmadi E, Gramlich R, Grützkau A, Hitzler M, Krüger M, Baumgrass R, et al. TLR2-  
709 activated human langerhans cells promote Th17 polarization via IL-1 $\beta$ , TGF- $\beta$  and IL-23. *Eur J*  
710 *Immunol.* 2009;39(5):1221–30.
- 711 66. Collin M, Bigley V. Human dendritic cell subsets: an update. *Immunology.* 2018;154(1):3–20.
- 712 67. Jurkin J, Krump C, Köffel R, Fieber C, Schuster C, Brunner PM, et al. Human skin dendritic  
713 cell fate is differentially regulated by the monocyte identity factor Kruppel-like factor 4 during  
714 steady state and inflammation. *J Allergy Clin Immunol.* 2017;139(6):1873-1884.e10.
- 715 68. Kim JH, Hu Y, Yongqing T, Kim J, Hughes VA, Le Nours J, et al. CD1a on Langerhans cells  
716 controls inflammatory skin disease. *Nat Immunol.* 2016;17(10):1159–66.
- 717 69. Luo Y, Cai X, Liu S, Wang S, Nold-Petry CA, Nold MF, et al. Suppression of antigen-specific  
718 adaptive immunity by IL-37 via induction of tolerogenic dendritic cells. *Proc Natl Acad Sci.*  
719 2014;111(42):15178–83.
- 720 70. Guttman-Yassky E, Zhou L, Krueger JG. The skin as an immune organ: Tolerance versus  
721 effector responses and applications to food allergy and hypersensitivity reactions. *J Allergy*  
722 *Clin Immunol.* 2019;S0091-6749(19):30474–9.

723

724

725

726

727

728

729

730

**Fig. 1. BMP7-driven LCs show up-regulation of inflammation-associated genes.**

(A) Schematic overview of *in vitro* LC generation from CD34<sup>+</sup> cord blood hematopoietic progenitor cells. Bright field images represent day 7 LC clusters. Flow cytometry contour plots represent day 7 expression of CD1a/CD207 induced by TGF- $\beta$ 1 or BMP7. (B) Heat map visualizes gene expression profiles of differentially expressed genes. CD1a<sup>+</sup>/CD207<sup>+</sup> LCs were generated from three independent donors in response to TGF- $\beta$ 1 or BMP7 and were FACS sorted before analysis. Colors represent high (red) and low (blue) intensity. (C) qRT-PCR analysis of TLR1-10 mRNA expression by day 7 generated MACS sorted LCs (TGF- $\beta$ 1 vs. BMP7). Values are normalized to HPRT (n=4,  $\pm$ SD, 2-tailed Student's t test, \*P<0.05; \*\* P<0.005). (D) Flow cytometry contour plots represent day 7 expression of TLR2 on CD207<sup>+</sup>LCs induced by TGF- $\beta$ 1 or BMP7. Graph represents mean fluorescence intensity (MFI) of TLR2 by CD207<sup>+</sup> cells (n=4,  $\pm$ SD, 2-tailed Student's t test, \*P<0.05). (E) MACS sorted LCs (TGF- $\beta$ 1-LCs or BMP7-LCs) were activated or not for 48h with 5 $\mu$ g/ml PGN and cytokine production was measured by cytokine array (right; n=3, 1-way ANOVA, corrected with Tukey multiple comparison test, \* P<0.05; \*\* P<0.005; \*\*\* P<0.005).

**Fig. 2. Immunophenotypic analysis of *in vitro* generated LCs.**

(A) Pre-expanded CD34<sup>+</sup> cells were cultivated for 7 days with GM-CSF, FLT3-L, SCF, TNF $\alpha$  and either TGF- $\beta$ 1 or BMP7. Histograms depict relative expression level of indicated markers for gated CD1a<sup>+</sup>/CD207<sup>+</sup> cells. Bars graphs represent mean fluorescence intensity (MFI) for listed markers (n=4, mean  $\pm$ SD, 2-tailed Student's t test, \* P<0.05; \*\* P<0.005; \*\*\* P<0.0005). (B) Phenotype of MACS sorted peripheral blood monocytes vs. CD1c<sup>+</sup> DCs. (C) CD14<sup>+</sup> peripheral blood monocytes were differentiated to LCs for 5 days with GM-CSF and either TGF- $\beta$ 1 or BMP7. Histograms depict relative expression level of CD1c and CD206 for gated CD1a<sup>+</sup>/CD207<sup>+</sup> cells (n=3). (D) CD1c<sup>+</sup> peripheral blood DCs were differentiated to LCs for 3 days with GM-CSF and either TGF- $\beta$ 1 or BMP7. Histograms depict relative expression level of CD1c and CD206 for gated CD1a<sup>+</sup>/CD207<sup>+</sup> cells (n=3). (E) CD34<sup>+</sup> cells-derived LCs were FACS sorted for CD207<sup>+</sup> cells, then fixed with

glutaraldehyde. Ultrathin sections were analyzed with Tecnai-20 transmission electron microscope (n=3). Size bars left = 2 $\mu$ m; right = 500nm.

**Fig. 3. The psoriatic epidermis harbours LCs with phenotypical resemblance to *in vitro* BMP7-driven LCs.** Representative images of sections from healthy adult human skin (A) and psoriatic lesions (B) were analyzed for the expression of CD207, CD1c and CD206. Arrow heads indicate triple positive CD207/CD1c/CD206 cells. Scatter plot (right) shows % of CD1c<sup>+</sup>CD206<sup>+</sup> cells in CD207<sup>+</sup> population (n=3, 2-tailed Student's *t* test, \*P<0.05). (C) Single cell suspension from biopsies of lesional skin of two psoriatic patients was analyzed with flow cytometry. After gating for singlets and viable cells, CD207<sup>+</sup> cell population has been assessed for the expression of CD1c, CD206, and TLR2. Scatter plot (right) shows % of CD1c<sup>+</sup>CD206<sup>+</sup>TLR2<sup>+</sup> cells in CD207<sup>+</sup> population (n=2). Representative images of sections from healthy adult human skin (D) and psoriatic lesions (E) were analyzed for the expression of BMPRII and CD207. Scatter plot (right) shows % CD207<sup>+</sup> co-expressing BMPRII (n=3). Nuclei were visualized with Dapi. The dotted lines represent the dermal–epidermal junction (n=3). Size bar=50 $\mu$ m.

**Fig. 4. BMP7-SMAD1/5/8 signaling is strongly induced in the psoriatic epidermis.** Representative images of paraffin sections from healthy adult human skin and psoriatic lesions were analysed for the expression of CD1a, BMP7 (A, B) and CD1a, phospho-SMAD1/5/8 (pSMAD1/5/8) (C, D). Nuclei were visualized with Dapi. The dotted lines represent the dermal–epidermal junction (n=3). Size bar = 50 $\mu$ m. (E) Representative images of sections from the ears of Junf/fJunBf/f K5cre-ERT mice (ctrl – cre- littermate control, KO d7 – Jun/JunB knockout day 7, KO d12 – Jun/JunB knockout day 14) analysed for the expression of BMP7, CD207 and phospho-SMAD1/5/8 (pSmad1/5/8). Nuclei were visualized with Dapi. The dotted lines represent the dermal–epidermal junction (n=5). (F) Schematic presentation of noggin (nog) and tamoxifen (Tx) treatment regiment of Junf/fJunBf/f K5cre-ERT mice. (G) Ear swelling in control and Jun/JunB KO animals intradermally injected with ctrl (0.1% BSA+beads) or noggin (nog+beads) n=5,  $\pm$ SEM, 1-way ANOVA, corrected with Tukey multiple comparison test, \* P<0.05. (H) Representative images of disease progression in nog (KO nog) and ctrl (KO ctrl) injected ears on experiment day 12. (I) Epidermal thickness in all experimental groups

assessed based on H&E staining (n=6,  $\pm$ SEM, 1-way ANOVA, corrected with Tukey multiple comparison test, \* P<0.05; \*\* P<0.005). **(J)** Ear skin histology (H&E, day 12) of control and Jun/JunB KO animals intradermally injected with ctrl (0.1% BSA) or noggin (nog). Size bar = 100 $\mu$ m

**Fig. 5. BMP7 supplementation is associated with mitotic activity of CD207<sup>+</sup> LC.**

**(A)** Pre-expanded CD34<sup>+</sup> cells were cultivated for 7 days with GM-CSF, FLT3-L, SCF, TNF $\alpha$  and either TGF- $\beta$ 1 or BMP7. Graph depicts proliferation (total cell number) at day 7 and day 14 (n=4, mean  $\pm$ SD, 2-tailed Student's t test, \*\* P<0.005). **(B)** Graph represents % of phenotypically defined cells generated as stated in A, and analyzed by flow cytometry for the expression of LC lineage markers CD1a, CD207, CD324 (n=4, 2-tailed Student's t test, \* P<0.05; \*\* P<0.005). **(C)** Immunofluorescent and immunohistochemical stainings represent sections of day 7 generated LC clusters analyzed for the expression of Ki67 and CD207. Size bar = 50 $\mu$ m (n=3). **(D)** % of Ki67<sup>+</sup> cells among total CD207<sup>+</sup> LCs. Each symbol represent one cluster (n=10, 2-tailed Student's t test, \*\*\*\* P<0.0001). **(E)** Representative images of sections from healthy adult human skin and psoriatic lesions were analyzed for the expression of BMP7, Ki67 and CD207. Nuclei were visualized with Dapi. The dotted lines represent the dermal-epidermal junction. Size bar = 50 $\mu$ m (n=3). **(F)** % of Ki67<sup>+</sup> LCs calculated from immunohistology sections from healthy and psoriatic skin. Each symbol represents one patient. **(G)** Pie charts depict % of CD207<sup>+</sup> cells confined to the KC layers expressing BMP7 in healthy (n=2, mean) and psoriatic skin (n=4, mean). Mean was calculated from immunohistological sections.

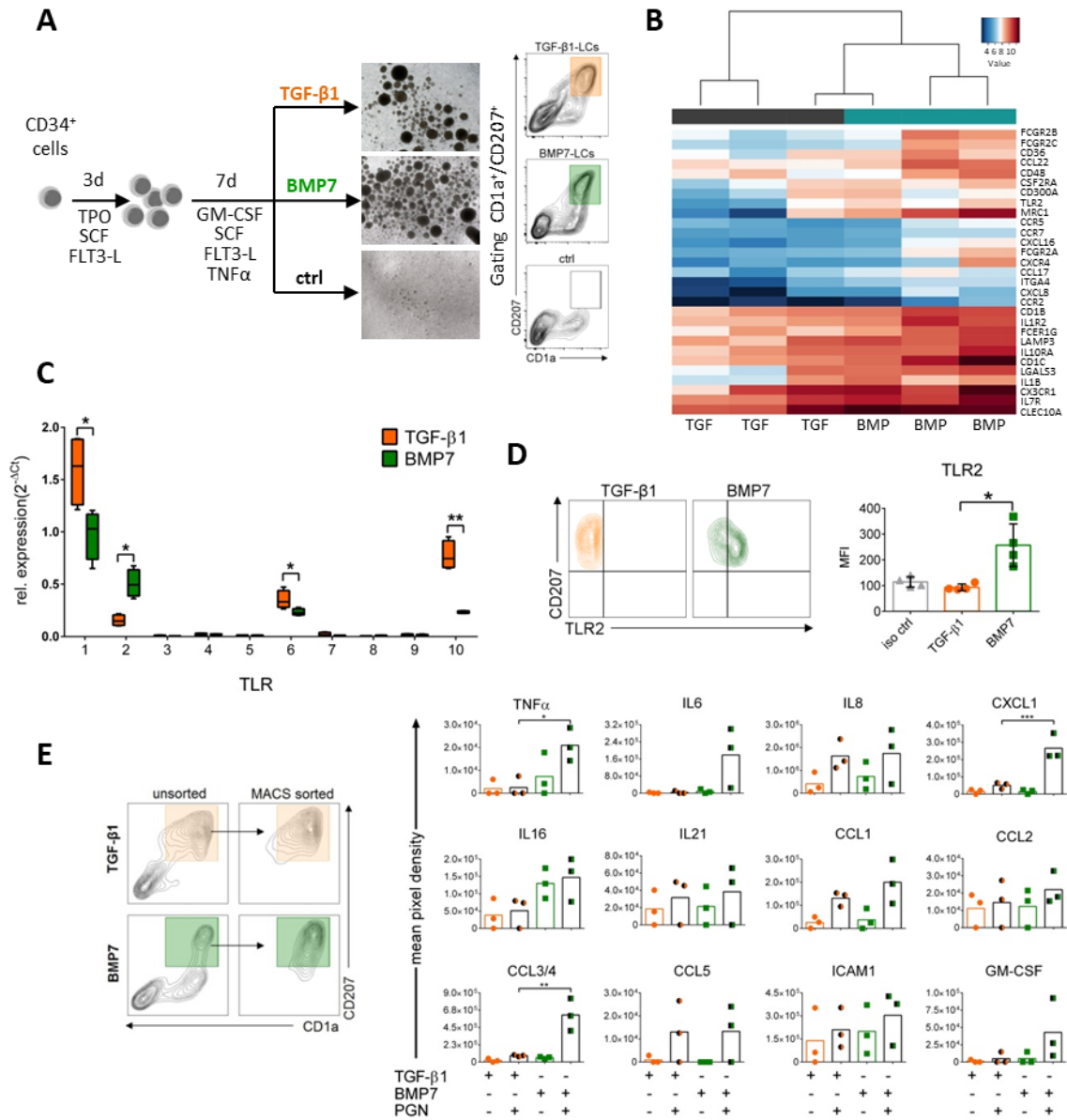
**Fig. 6. TGF- $\beta$ 1 represses BMP7-driven CD206<sup>+</sup>CD1c<sup>+</sup> LC characteristics via ALK5.**

**(A)** Schematic representation of canonical TGF- $\beta$ /BMP7 downstream signaling. **(B)** CD34<sup>+</sup> cells were induced to differentiate into LCs in the presence of TGF- $\beta$ 1 or BMP7 for 8 days. Parallel day 6 cultures were supplemented with BMP7 or TGF- $\beta$ 1 as indicated. Representative contour plots show expression of CD1c vs CD206 by gated day 8 generated CD1a<sup>+</sup>CD207<sup>+</sup> cells. Bars represent mean fluorescence intensity (MFI) of CD1c/CD206 for gated CD1a<sup>+</sup>/CD207<sup>+</sup> cells (n=3,  $\pm$ SD). **(C)** CD34<sup>+</sup> cells were cultured for 4 days, then pre-treated or not with SB421543 (ALK5 inhibitor) for 1 h,

Journal Pre-proof

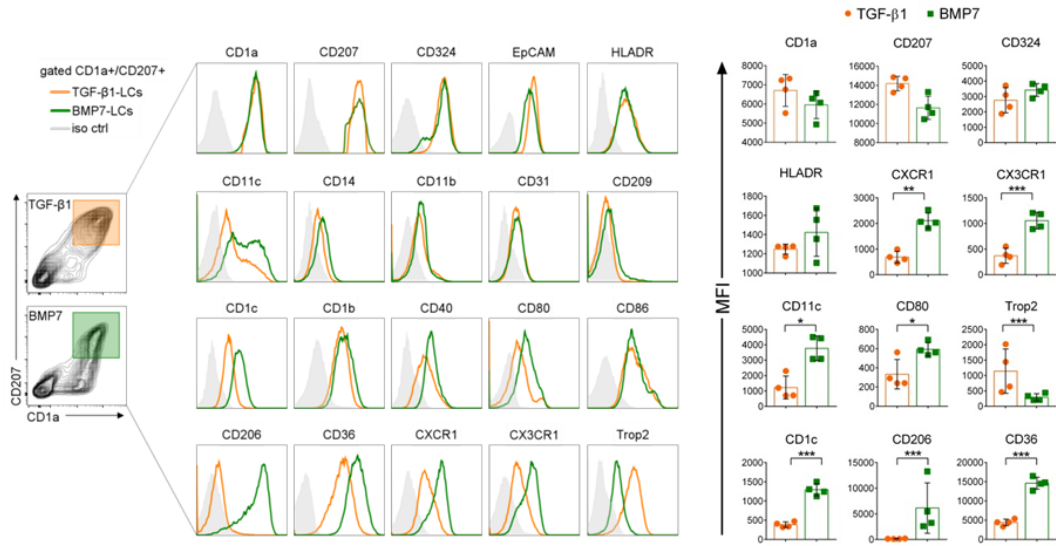
followed by TGF- $\beta$ 1 addition. Representative contour plots show day 7 generated gated CD1a<sup>+</sup>CD207<sup>+</sup> cells analyzed for the expression of CD1c and CD206. Bars represent mean fluorescence intensity (MIF) of CD1c/CD206 expression by gated CD1a<sup>+</sup>/CD207<sup>+</sup> cells pretreated or not with 8 $\mu$ M ALK5 inhibitor (n=3,  $\pm$ SEM, 2-tailed Student's *t* test, \* P<0.05; \*\* P<0.005).

**Fig. 7. Reduction in lesional epidermal BMP7 expression in psoriasis correlates with clinical improvement.** (A) Graph indicates relative staining intensity of BMP7 before and after dithranol treatment analyzed using ImageJ software (n=6, 2-tailed Student's *t* test, \* P<0.05). Representative images of sections from the lesional skin of psoriatic patients analyzed for the BMP7 expression before and after dithranol treatment. Size bar = 50 $\mu$ m. (B) Correlation between PASI score reduction and BMP7 relative staining intensity reduction after dithranol treatment (n=6, nonparametric Spearman correlation).

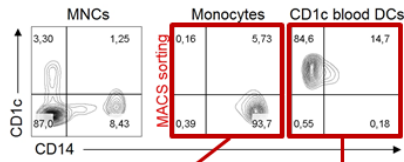




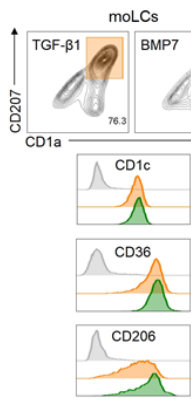
**A**



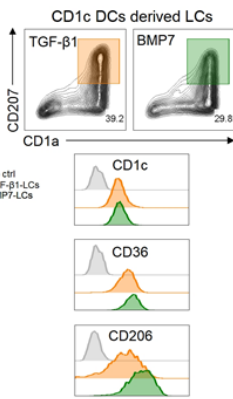
**B**



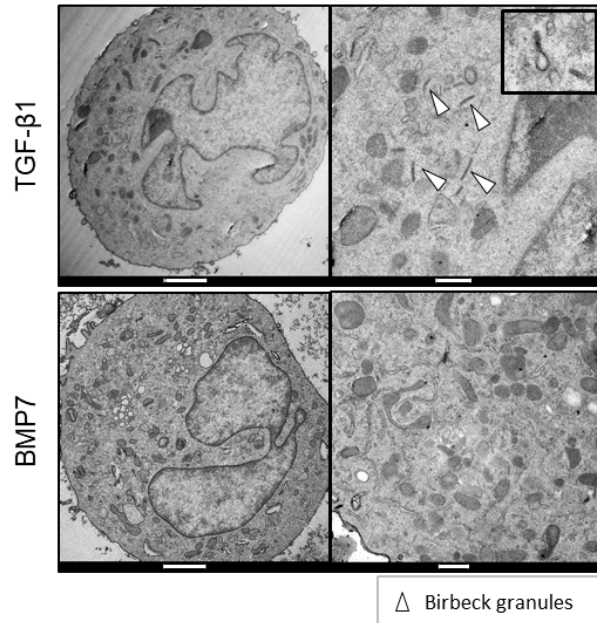
**C**

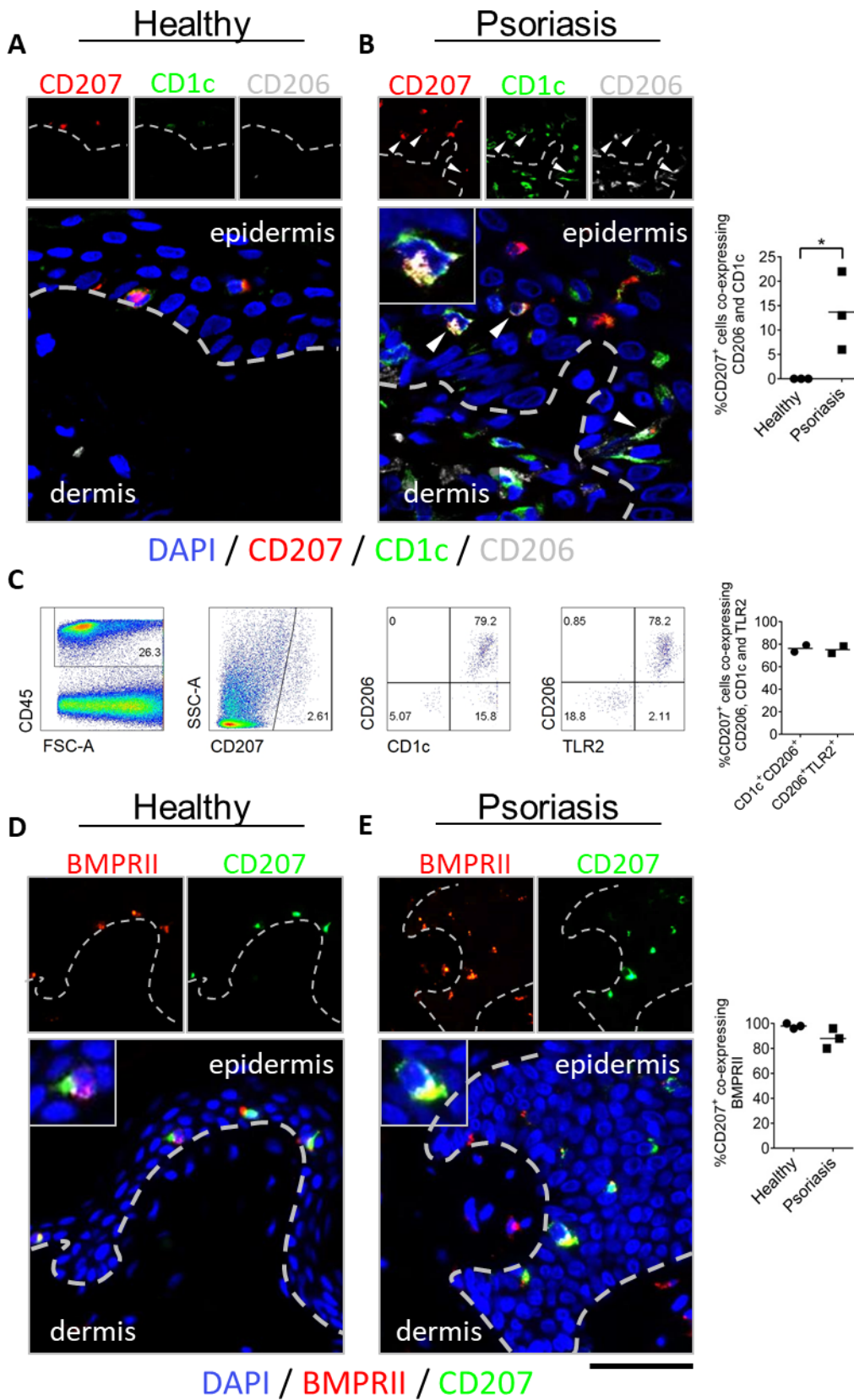


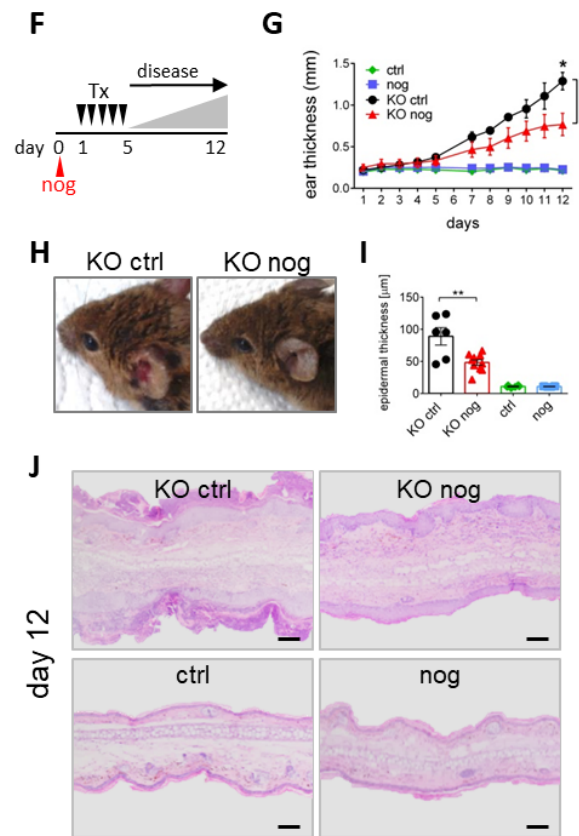
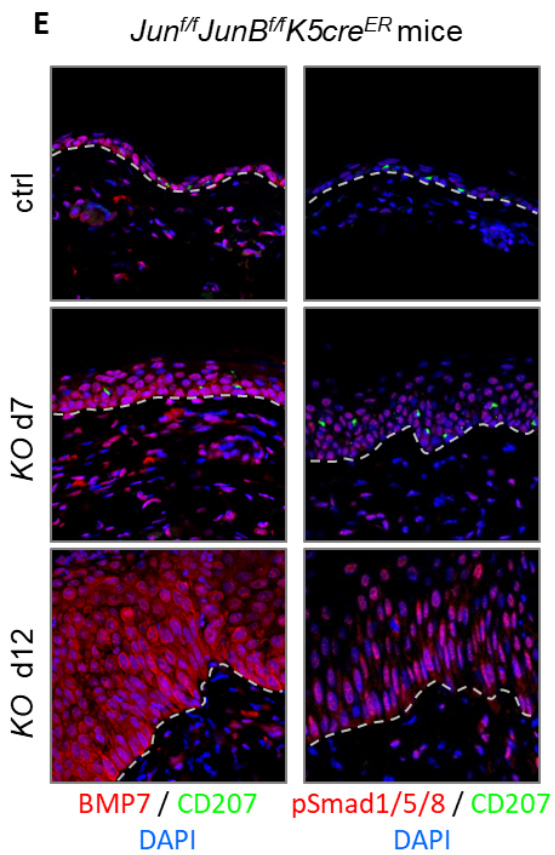
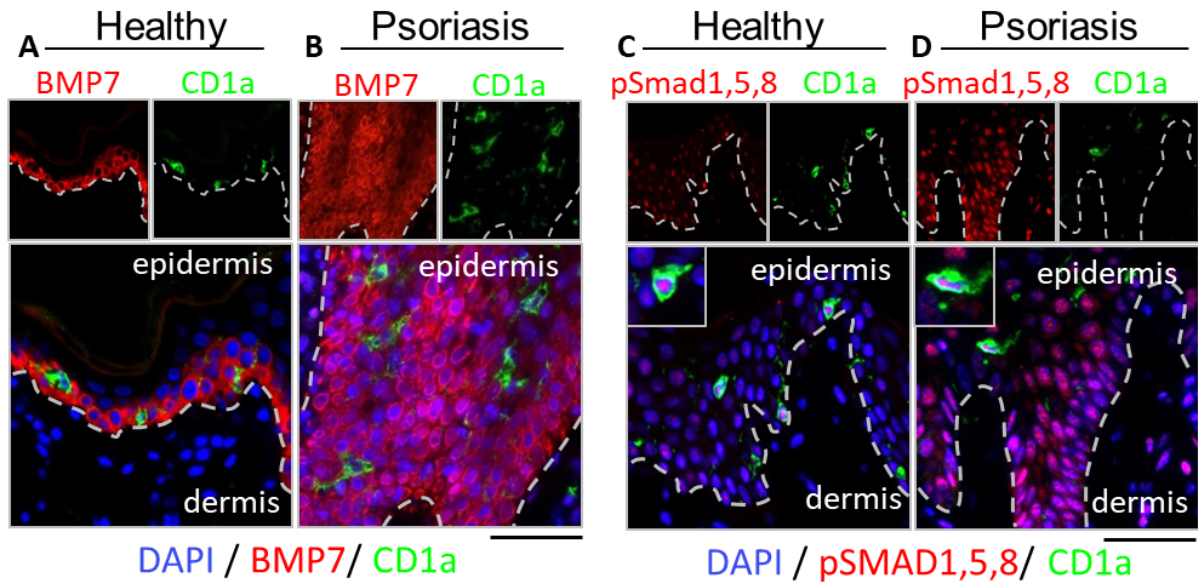
**D**

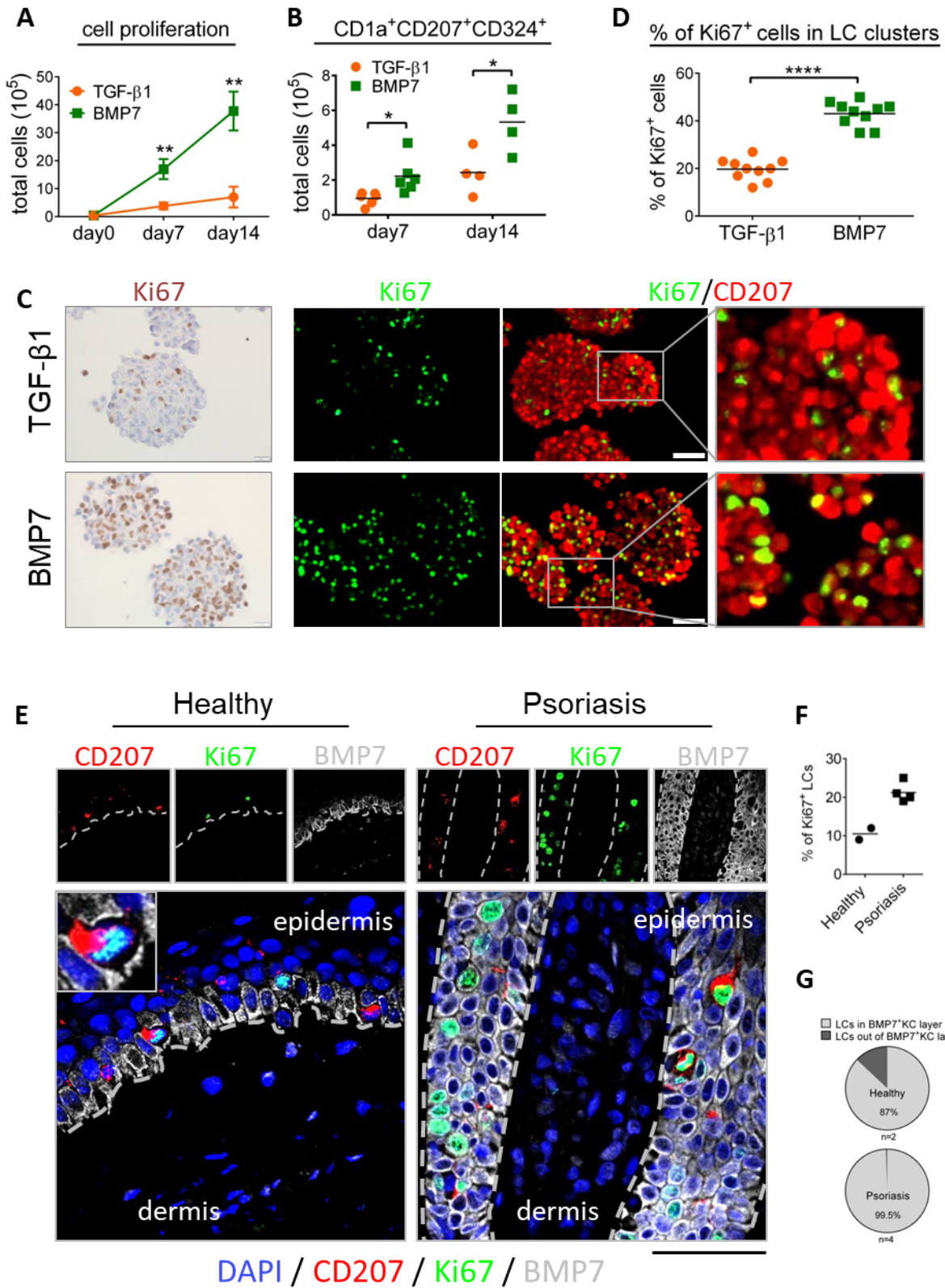


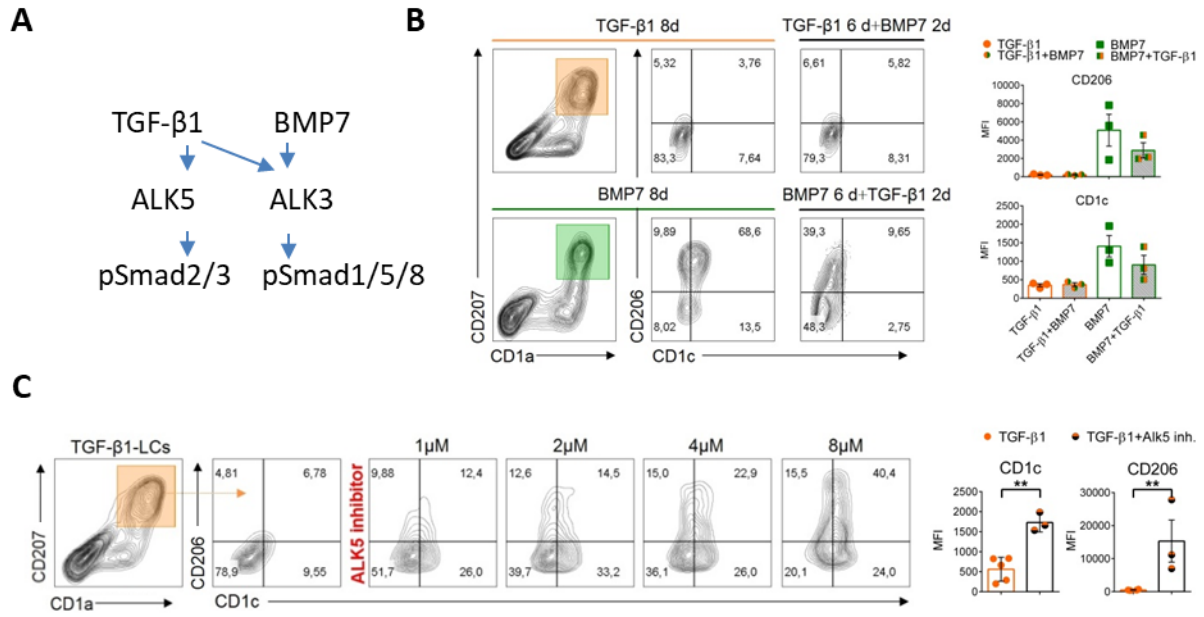
**E**

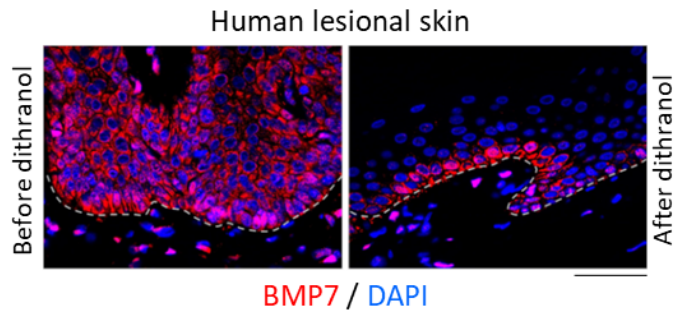
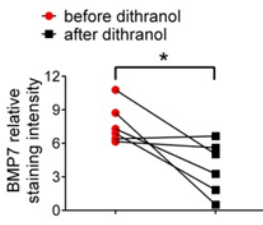
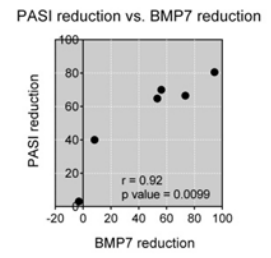




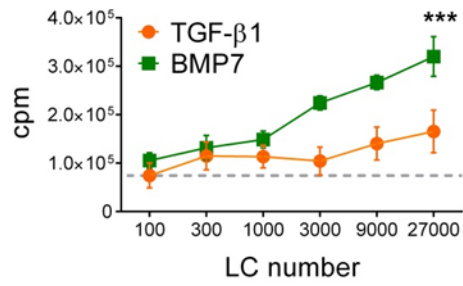




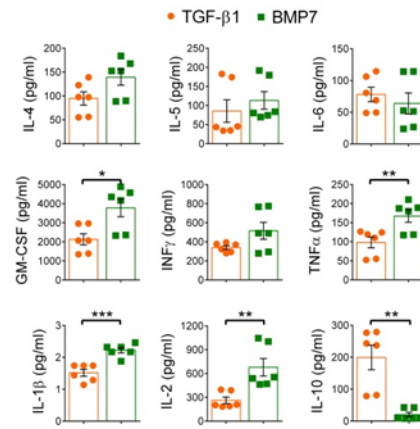


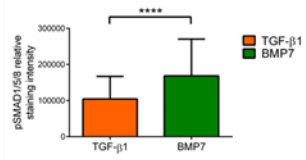
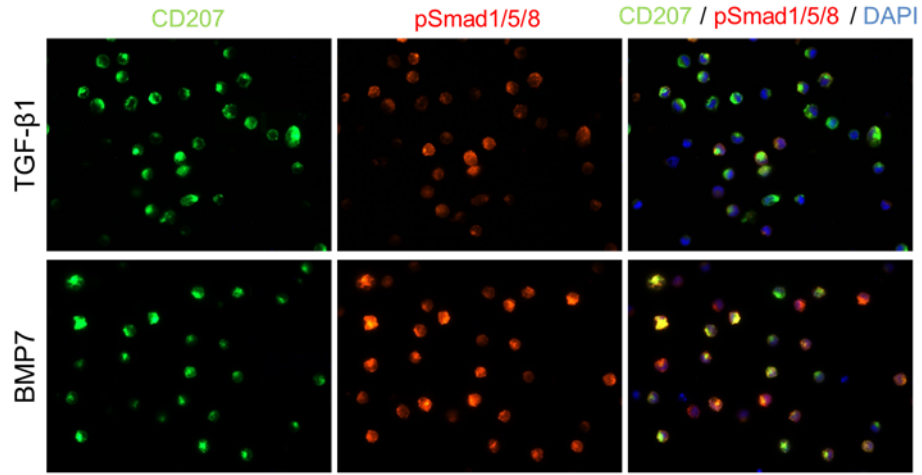
**A****B**

A

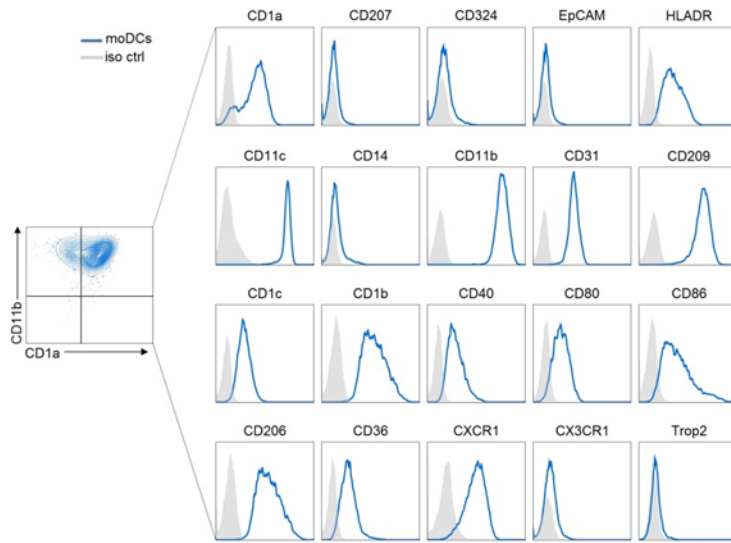


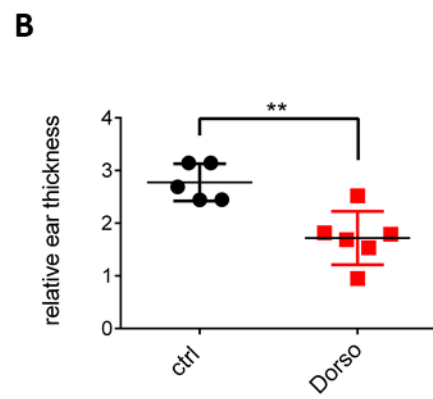
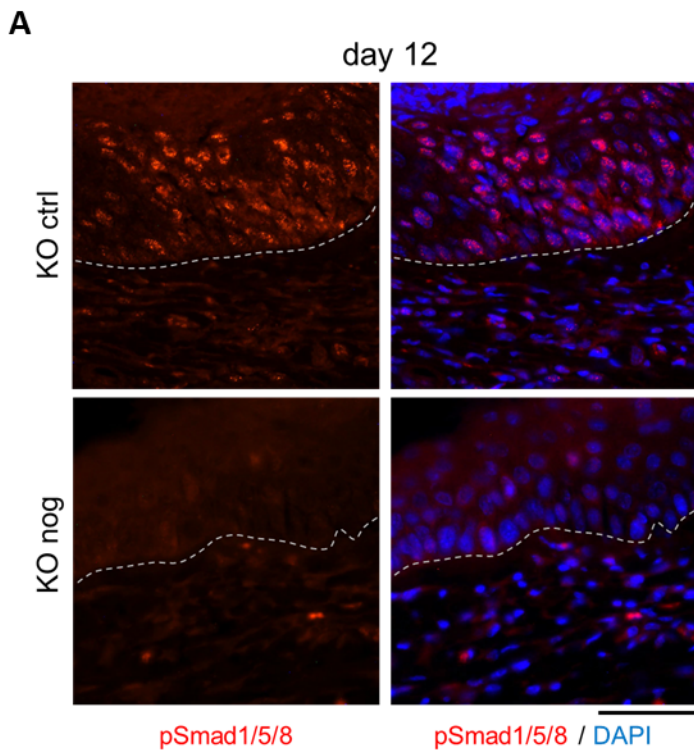
B

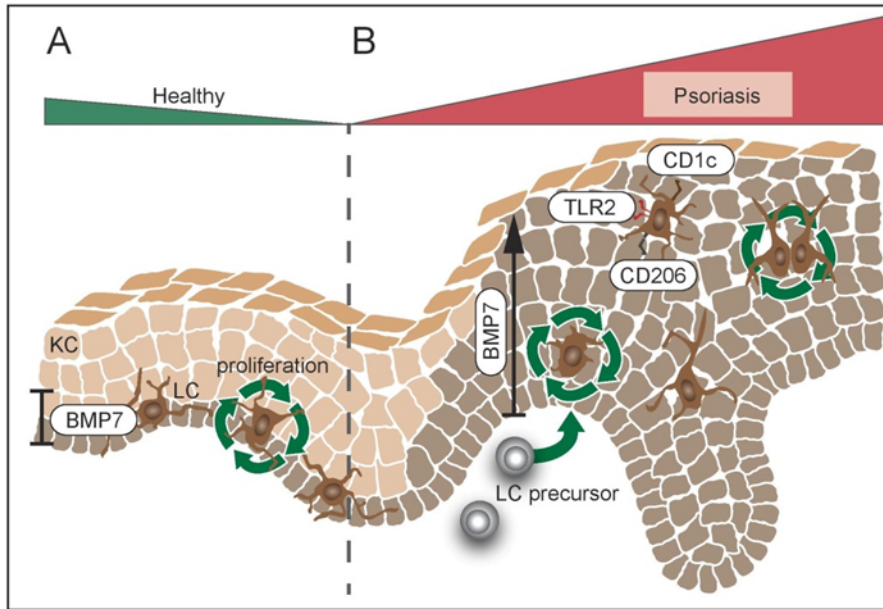






monocyte-derived DCs





**Supplemental material**

2

**Supplementary figure legends**

Fig. S1. BMP7-generated LCs exhibit immunostimulatory capacity

Fig. S2. BMP7-LCs express higher levels of pSmad1/5/8 than TGF- $\beta$ 1-LCs

Fig. S3. BMP7-LCs have a unique phenotype distinct from moDCs

Fig. S4. Inhibition of BMP signaling with noggin or Alk3 inhibitor results in decreased ear swelling *in vivo*

Fig. S5. Hypothetical model of pathogenic epidermal BMP signaling in psoriasis

10

**Supplementary methods**

Cell isolation

Preparation of single cell suspension from psoriatic skin biopsies

Gene expression analysis

RNA isolation, reverse transcription (RT-PCR) and real-time quantitative PCR (qPCR)

Cytokine measurements

Transmission electron microscopy (TEM)

Immunofluorescence and immunohistochemistry

Mice

Intradermal noggin injections in mice

Topical treatment with dorsomorphin

Murine skin thickness measurement

T-cell proliferation assay (MLR)

24

**Supplementary tables**

Table S1. Flow cytometry antibodies

Table S2. Cytokines and reagents

28 Table S3. qPCR primer sequences

29 Table S4. Immunohistology antibodies

30

31 **Supplementary references**

32

33

34

35

36

37

38

39

40

41

42

43

44

45

46

47

48

49

50

51

Journal Pre-proof

52 **Supplementary figure legends**

53

54 **Fig. S1. BMP7-generated LCs exhibit immunostimulatory capacity.**

55 (A)  $10^5$  naïve CD4 T cells were stimulated with the indicated numbers of LCs. Proliferation of T cells  
56 was monitored on day 5 of co-culture by addition of [methyl-3H]TdR, followed by measurement of  
57 [methyl-3H]TdR incorporation 18h later (n=3,  $\pm$ SD, 2-tailed Student's t test, \*\*\* P<0.0005). (B)  
58 Allogeneic, naïve CD4<sup>+</sup> T-cells were co-cultured for 5 days with TGF- $\beta$ 1- or BMP7-LCs. Cytokines in  
59 the supernatants were measured by Luminex system (n=6,  $\pm$ SEM, 2-tailed Student's t test P<0.05; \*\*  
60 P<0.005; \*\*\* P<0.0005).

61

62 **Fig. S2. BMP7-LCs express higher levels of pSmad1/5/8 than TGF- $\beta$ 1-LCs.**

63 Day 7 TGF- $\beta$ 1- and BMP7-LCs were MACS sorted. Cytospins were immunolabeled to assess CD207<sup>+</sup>  
64 cells for the expression of pSMAD1/5/8. Graph indicates relative staining intensity of pSmad1/5/8  
65 analyzed using ImageJ software. For the relative fluorescence intensity 150 CD207<sup>+</sup> cells/condition  
66 were measured (n=3, 2-tailed Student's t test, \*\*\*\* P<0.0001).

67

68 **Fig. S3. BMP7-LCs have a unique phenotype distinct from moDCs.** CD14<sup>+</sup> peripheral blood  
69 monocytes were differentiated for 7 days with GM-CSF and IL-4 to moDCs. Histograms depict  
70 relative expression level of indicated markers for CD1a<sup>+</sup>/CD11b<sup>+</sup> cell population (n=4).

71

72 **Fig. S4. Inhibition of BMP signaling with noggin or Alk3 inhibitor results in decreased ear**

73 **swelling *in vivo*.** (A) Representative images of sections from the ears of *Jun<sup>ff</sup>JunB<sup>ff</sup>K5cre-ER<sup>T</sup>* knock  
74 out mice injected intradermally (day 0) with beads-adsorbed noggin (KO nog) or 0.1% BSA + beads  
75 control (KO ctrl). Samples were analyzed for the expression of phospho-Smad1/5/8 (pSmad1/5/8) on  
76 day 12 of the experiment. Nuclei were visualized with Dapi. The dotted lines represent the dermal-  
77 epidermal junction (n=3). (B) *Jun<sup>ff</sup>JunB<sup>ff</sup>K5cre-ER<sup>T</sup>* knock out mice were treated topically from day  
78 10 of the experiment, with 10uM dorsomorphin (Dorso) for 5 consecutive days. Graph represents  
79 differences in ear thickness measured on day 15 (n=5-6, 2-tailed Student's t test, \*\*P<0.005).

**80 Fig. S5. Hypothetical model of pathogenic epidermal BMP signaling in psoriasis.**

81 BMP7 is expressed aberrantly throughout all KC layers in the lesional psoriatic epidermis and  
82 promotes the generation of proliferative  $CD206^+CD1c^+TLR2^+$ LCs from precursors. These psoriatic  
83 LCs occur scattered throughout the enlarged epidermis. Conversely, in the healthy epidermis, LCs are  
84  $CD206^-TLR2^-CD1c^{low/-}$ , exhibit a predominant basal/suprabasal location, and the occasionally  
85 observed mitotic LCs are confined to the basal  $BMP7^+$  KC layer. In psoriasis, aberrantly activated  
86 canonical BMP-pSMAD1/5/8 signaling promotes lesion formation and induces the generation of  
87 inflammatory LCs, sensitized for bacterial signaling. Our data suggest that aberrant high BMP7 in  
88 psoriatic KCs is mediated by a KC intrinsic process and enhances microbial signals in psoriatic  
89 lesions.

90

91

92

93

94

95

96

97

98

99

100

101

102

103

104

105

106

107

**Supplementary methods**

109

**Cell isolation**

111 CD34<sup>+</sup> hematopoietic progenitor/stem cells (HSCs):. Cord blood was collected during healthy, full-  
112 term deliveries. Ethics approval (26-520) was obtained from the Medical University of Graz  
113 Institutional Review Board for these studies. Informed consent was provided to patients in accordance  
114 with the Declaration of Helsinki. Cord blood CD34<sup>+</sup> HSCs were positively selected with magnetic  
115 sorting (EasySep<sup>TM</sup> Human CD34 Positive Selection Kit, StemCell Technologies<sup>TM</sup>). CD14<sup>+</sup>  
116 monocytes, naïve CD4<sup>+</sup> T-cells, CD1c<sup>+</sup> blood DCs: Buffy coats from healthy donors were purchased  
117 from Transfusion Medicine Department, Medical University of Graz, Austria. For the isolation of  
118 peripheral blood mononuclear cells (PBMCs) heparinized blood was separated by gradient  
119 centrifugation with Lymphoprep<sup>TM</sup> (Axis Shield, Norway). Subsequently, various cells were isolated  
120 using magnetic sorting technique according to the manufacturer's instructions. First, CD14<sup>+</sup> monocytes  
121 were positively selected (CD14 MicroBeads, human, Miltenyi Biotec, Germany). Second, after  
122 depletion of CD19<sup>+</sup> cells, CD1c<sup>+</sup> blood dendritic cells were positively selected (CD1c<sup>+</sup>/BDCA-1  
123 Dendritic Cell Isolation Kit, human, Miltenyi Biotec, Germany). Last, naïve CD4<sup>+</sup> T-cells were  
124 negatively selected (MagniSort<sup>TM</sup> Human CD4 Naïve T cell Enrichment Kit, ThermoFisher Scientific,  
125 USA). Purity of sorted cells was assessed by flow cytometry and was greater than 95%.

126

**Preparation of single cell suspension from psoriatic skin biopsies**

128 Punch biopsies (4 mm) have been taken from lesional skin of psoriatic patients. Ethics approval  
129 (EK700/2009) was obtained from the Medical University of Vienna Institutional Review Board for  
130 these studies. Informed consent was provided to patients in accordance with the Declaration of  
131 Helsinki. To prepare single cell suspension gentleMACS<sup>TM</sup> Dissociator (Miltenyi Biotec, Germany)  
132 have been used. Skin biopsy was cut into small pieces and transferred into gentleMACS C Tube  
133 (Miltenyi Biotec, Germany) containing mix of 900 µl Collagenase IV (0.5 Wunsch units/ml) and 100  
134 µl DNase I (10 mg/ml). Tissue with enzymes was incubated overnight in 37°C in shaking water bath.  
135 This was followed by tissue disassociation using gentleMACS<sup>TM</sup> Dissociator system. Obtained cell



136 suspension was filtered through 100  $\mu\text{m}$  cell strainer and centrifuged for 10 min in 4°C at 1600 rpm.  
137 After supernatant was discarded cell pellet was stained for flow cytometry analysis.

138

### 139 **Gene expression analysis**

140 The raw data of the dataset GSE49085 (1) (6 samples, Affymetrix Human Genome U133 Plus 2.0  
141 Array) was downloaded from Gene Expression Omnibus (2) and analysed in  
142 R 3.5.1 (<https://www.R-project.org>). The R package 'oligo' (3) was used for quality control and  
143 pre-processing. The R package 'limma' (4) was used to calculate log<sub>2</sub> (fold changes) and p values  
144 between the groups with patients as covariates. Specific filtering was applied using selected  
145 features associated with dendritic cells (24). The p-values were adjusted for multiple testing with  
146 Benjamini and Hochberg's method to control the false discovery rate. Genes with an absolute  
147 log<sub>2</sub>(fold change) > log<sub>2</sub>(1.5) and an adjusted p-value  $\leq 0.05$  were considered as differentially  
148 expressed. Hierarchical clustering with Euclidean distance and Ward linkage was performed and  
149 visualized as a heatmap. The heatmap was generated using the R package 'gplots'.

150

### 151 **RNA isolation, reverse transcription (RT-PCR) and real-time quantitative PCR (qPCR)**

152 Prior to the RNA extraction, day 7 CD207<sup>+</sup> cells were isolated with magnetic sorting (human  
153 CD207/Langerin MicroBeads, Miltenyi Biotec, Germany). Extraction of total RNA from sorted LCs  
154 (purity  $\geq 80\%$ ) was performed with RNeasy Micro Kit (Qiagen, Germany). cDNA was generated  
155 using High-Capacity cDNA Reverse Transcription Kit (Applied Biosystems, USA). The qPCR was  
156 performed using Fast SYBR<sup>TM</sup> Green Master Mix (Applied Biosystems, USA) and CFX96 Real-Time  
157 Thermal cycler (Bio-Rad Laboratories, USA). All steps were performed according to the  
158 manufacturer's instructions. Values were normalized to HPRT. Primer sequences are listed in the  
159 supplementary table 2.

160

### 161 **Cytokine measurements**

162 Day 7 CD207<sup>+</sup> LCs (TGF- $\beta$ 1-LCs vs. BMP7-LCs) were MACS sorted (purity  $\geq 90\%$ ) and activated  
163 with 5  $\mu\text{g}/\text{ml}$  PGN. After 48h supernatants were collected. The proteome profiler human cytokine  
164 array kit (R&D Systems, USA) was used according to the manufacturer's instructions. Spot intensity

165 was quantified with ImageLab™ software (BioRad). For the quantitative measurement of cytokines in  
166 the supernatants from T-cell/LC co-culture experiments Luminex system was used.

167

### 168 **Transmission electron microscopy (TEM)**

169 Day 7 FACS sorted CD207<sup>+</sup> LCs were fixed with 2,5% Glutaraldehyde and 1% OsO<sub>4</sub> palade and  
170 dehydrated in a graded ethanol series. Afterward, LCs were embedded in Epon (Serva, Germany) and  
171 ultrathin sections (70–100 nm) were cut using an UltraCut-UCT ultramicrotome (Leica Inc., Austria),  
172 transferred to copper grids, and viewed either unstained or stained with 1% uranyl acetate and 5% lead  
173 citrate (Merck, Germany) using a Tecnai-20 TEM (Tecnai-20 equipped with a LaB6 cathode; FEI  
174 Company, Netherlands) at an acceleration voltage of 80 kV. Digital images were recorded with an  
175 Eagle 4 k-CCD camera; chip size: 4,096 × 4,096 pixels (FEI Company).

176

### 177 **Immunofluorescence and immunohistochemistry**

178 Healthy, adult (18-42 year) skin samples were collected after plastic surgery. Ethics approval (27-071)  
179 was obtained from the Medical University of Graz Institutional Review Board for these studies.  
180 Informed consent was provided to patients in accordance with the Declaration of Helsinki. Paraffin  
181 sections (4µm) were subjected to HIER antigen retrieval in Target Retrieval Solution pH 6.0  
182 (Agilent/Dako, USA) followed by blocking with 5% donkey serum (Jackson ImmunoResearch  
183 Laboratories, USA). Primary and secondary antibodies are listed in the supplementary table 4.  
184 Staining specificity controls were performed with substitution of primary antibodies by isotype-  
185 matched control antibody against irrelevant antigens followed by corresponding secondary antibody.  
186 To visualize nuclei, sections were counterstained with 10µg/mL DAPI. Images were obtained with  
187 Leica DM4000B microscope and ZEIS LSM700 confocal microscope and processed using LAS V3.8,  
188 ZEN 2.3 lite, and ImageJ software.

189

### 190 **Mice**

191 *Jun<sup>ff</sup>JunB<sup>ff</sup> K5cre-ER<sup>T</sup>* mice (mixed background) with conditional deletion of Jun/JunB under keratin  
192 5 promoter (K5cre-ERT) were described previously (5). To delete Jun/JunB K5-cre<sup>ER</sup> positive (KO) or  
193 negative (ctrl; *Jun<sup>ff</sup>JunB<sup>ff</sup>*) mice were injected intraperitoneally with 1 mg tamoxifen (Tx, Sigma-

194 Aldrich, USA) in an emulsion with sunflower seed oil (Sigma-Aldrich)/ethanol mixture (10:1) on 5  
195 consecutive days. Deletion of Jun/JunB was verified by PCR. Mice were kept in the animal facility of  
196 the Medical University of Vienna in accordance with institutional policies and federal guidelines.  
197 Animal experiments were approved by the Animal Experimental Ethics Committee of the Medical  
198 University of Vienna and the Austrian Federal Ministry of Science and Research. (Animal license  
199 numbers: GZ 66.009/124-BrGT/2003; GZ 66.009/109-BrGT/2003; BMWF-66.009/0073-II/10b/2010  
200 BMWF-66.009/0074-II/10b/2010; BMWFW-66.009/0200-WF/II/3b/2014; and BMWF W-  
201 66.009/0199-WF/II/3b/2014).

202

### 203 **Intradermal noggin injections in mice**

204 For delivery of Noggin-adsorbed beads, we used a previously described approach (6–9). Ears of  
205 *Jun<sup>fl/fl</sup>JunB<sup>fl/fl</sup>K5cre-ER<sup>T</sup>* mice were injected intradermally one time with a mix of FluoSpheres®  
206 (Invitrogen, USA) and noggin (300ng) 24h before Tx injection. For control challenge injection a mix  
207 of FluoSpheres® and 0.1% BSA was used.

208

### 209 **Topical treatment with dorsomorphin**

210 *Jun<sup>fl/fl</sup>JunB<sup>fl/fl</sup>K5-cre-ER<sup>T</sup>* mice aged 5-6 weeks were injected with Tamoxifen (Tx) to trigger psoriasis  
211 as previously published (5,10) After five consecutive days of Tx injection, mice were given an  
212 additional 5 days to manifest a pronounced phenotype. After this, for another five consecutive days  
213 inhibitors were applied topically to the ears of the mice. Dorsomorphin (Tocris Bioscience, UK) was  
214 diluted to a concentration of 10 $\mu$ M in DMSO; of this mixture, 40 $\mu$ L were pipetted onto each mouse  
215 ear (20 $\mu$ l to the dorsal, 20 $\mu$ l to the ventral side). The control group received pure DMSO. Ear  
216 thickness was measured daily via caliper. After five days of treatment (from day 10 to 15), the increase  
217 of ear thickness relative to ear thickness at the start of inhibitor treatment was calculated.

218

### 219 **Murine skin thickness measurement**

220 Paraffin sections from mouse ears were stained with hematoxylin and eosin (Sigma, USA). Images  
221 were obtained with Olympus BX53 (Olympus) microscope. Epidermal thickness was measured in 20

222 random fields on 5 independent pictures per sample (magnification 10x) using AxioVision LE64  
223 software (Zeiss).

224

### 225 **T-cell proliferation assay (MLR)**

226 The assay was performed as described previously (11). In brief, MACS-sorted CD207<sup>+</sup> LCs were  
227 seeded in graded numbers with a constant number ( $5 \times 10^5$ ) of purified, allogenic naive CD4<sup>+</sup> T-cells in  
228 96-well tissue culture plates in RPMI-1640 medium (Sigma-Aldrich, USA) supplemented with 10%  
229 FBS. The proliferation of T-cells was analyzed on day 5 of culture by adding [methyl-<sup>3</sup>H]TdR  
230 followed by incorporation measurement [methyl-<sup>3</sup>H]TdR 18h later. Incorporated radioactivity was  
231 measured using a 1450 microbeta plate reader (Wallac-Trilux Instrument; Life Science). Supernatants  
232 were collected for cytokine measurement (Luminex) before adding [methyl-<sup>3</sup>H]TdR. Assays were  
233 performed in triplicates.

234

235

236

237

238

239

240

241

242

243

244

245

246

247

248

249

250

251 **Supplementary tables**

252

<b>Antibody (anti-)</b>	<b>Clone</b>	<b>Company</b>
CD1a	HI149	BD Biosciences
CD1b	SN13(K5-1B8)	BioLegend
CD1c	510/21A3	BD Biosciences
CD11b	ICRF44	BioLegend
CD11c	BU15	BioLegend
CD14	M5E3	BioLegend
CD31	WM59	BioLegend
CD36	CB38	BD Biosciences
CD40	5C3	BD Biosciences
CD80	L307.4	BD Biosciences
CD86	2331(FUN-1)	BD Biosciences
CD206	15-2	BioLegend
CD207	DCGM4	Beckman Coulter
CD209	eB-h209	eBioscience
CD324/E-cadherin	67A4	BD Biosciences
CXCR1	8F1-CXCR1	BioLegend
CX3CR1	2A9-1	eBioscience
HLADR	G46-6	BD Biosciences
EpCAM/Trop1	EBA-1	BD Biosciences
Trop2	162-46	BD Biosciences
TLR2	1167	BD Biosciences

253

254 **Table S1. Flow cytometry antibodies**

255

256

257

258

259

260

261

262

263

264

265

Cytokine/reagent	Company
Trombopoietin (TPO)	PeproTech, UK
Stem cell factor (SCF)	
Fms-related tyrosine kinase 3 ligand (FLT3-L)	
Tumor necrosis factor alpha (TNF $\alpha$ )	
Granulocyte-macrophage colony-stimulating factor (GM-CSF)	
Interleukin 4 (IL-4)	R&D Systems, USA
Transforming growth factor beta 1 (TGF- $\beta$ 1)	
Recombinant mouse noggin (NOG)	ImmunoTools, Germany
Bone morphogenetic protein 7 (BMP7)	
Alk4/5/7 inhibitor (SB431542)	Tocris Bioscience, UK
Dorsomorphin	
FluoSpheres® carboxylate-modified microspheres 0.2 $\mu$ m, crimson fluorescent (625/645) 2% solids	Invitrogen, USA
Recombinant extracellular domain of Notch ligand Delta-1 (Delta-1 <sup>ext</sup> -IgG)	Kindly provided by I. Bernstein

266

267 **Table S2. Cytokines and reagents**

268

269

270

271

272

273

274

275

276

277

278

279

280

281

282

283

Name	Orientation	Sequence 5'→3'
TLR1	fw	GGCACCCCTACAAAAGGAATC
	rev	TGAAGATAATGGCAAAATGGAAG
TLR2	fw	GCTGCCATTCTCATTCTTCTG
	rev	GCCACTCCAGGTAGGTCTTG
TLR3	fw	TCCACCACCAGCAATACAAC
	rev	AAGCCAAGCAAAGGAATCG
TLR4	fw	TCATTGTCCTGCAGAAGGTG
	rev	AGATGTTGCTTCCTGCCAAT
TLR5	fw	TTGCTCAAACACCTGGACAC
	rev	CACCACCATGATGAGAGCAC
TLR6	fw	GACCTACCGCTGAAAACCAA
	rev	CTCACAATAGGATGGCAGGA
TLR7	fw	TCCTAAAACCTCTGCCCTGTGA
	rev	GGGAGATGTCTGGTATGTGG
TLR8	fw	GGGGATCAAAGAGGGAAGAG
	rev	TTGGGATGTGGAAAGAGACC
TLR9	fw	CTGCCTTCCTACCCTGTGAG
	rev	AGAATCATGGAGGTGGTGA
TLR10	fw	TGGTTGGATGGTCAGATTCA
	rev	AGGGCAGATCAAAGTGGAGA
HPRT	fw	GACCAGTCAACAGGGGACAT
	rev	AACACTTCGTGGGGTCCTTTTC

284

285 **Table S3. qPCR primer sequences**

286

287

288

289

290

291

292

293

294

295

296

297

298 **pAb** – polyclonal antibody  
 299 **mAb** – monoclonal antibody  
 300

<b>Primary antibody</b>	<b>Clone</b>	<b>Company</b>
pAb rabbit anti-CD207	N/A	Sigma-Aldrich, USA
mAb rat anti-CD207 Alexa Fluor-488	929F3.01	Dendritics, France
pAb rabbit anti-BMP7	N/A	LifeSpan BioSciences, USA
mAb mouse anti-Ki67	MIB-1	Dako, USA
pAb rabbit anti-pSMAD1/5/8	N/A	CellSignaling, USA
mAb mouse anti-CD1a	O10	Novus Biologicals, USA
mAb mouse anti-CD1c	OT12F4	Abcam, UK
pAb rabbit anti-CD206	N/A	Sigma-Aldrich, USA
pAb rabbit anti-BMPR2	N/A	

#### **Secondary antibody (conjugated)**

pAb donkey anti-mouse DyLight488	N/A	Jackson ImmunoResearch Laboratories, USA
pAb donkey anti-mouse Cy3	N/A	
donkey anti-rabbit Cy3	N/A	
donkey anti-rabbit DyLight488	N/A	
donkey anti-rabbit Alexa Fluor-647	N/A	

301

302 **Table S4. Immunohistology antibodies**

303

304

305

306

307

308

309

310

311

312

313

314

315

316

317

318



319 **Supplementary references**

- 320 1. Yasmin N, Bauer T, Modak M, Wagner K, Schuster C, Köffel R, et al. Identification of bone  
321 morphogenetic protein 7 (BMP7) as an instructive factor for human epidermal Langerhans cell  
322 differentiation. *J Exp Med*. 2013;210(12):2597–610.
- 323 2. Edgar R, Domrachev M, Lash AE. Gene Expression Omnibus: NCBI gene expression and  
324 hybridization array data repository. *Nucleic Acids Res*. 2002;30(1):207–10.
- 325 3. Carvalho BS, Irizarry RA. A framework for oligonucleotide microarray preprocessing.  
326 *Bioinformatics*. 2010;26(19):2363–7.
- 327 4. Ritchie ME, Phipson B, Wu D, Hu Y, Law CW, Shi W, et al. Limma powers differential  
328 expression analyses for RNA-sequencing and microarray studies. *Nucleic Acids Res*.  
329 2015;43(7):e47.
- 330 5. Zenz R, Eferl R, Kenner L, Florin L, Hummerich L, Mehic D, et al. Psoriasis-like skin disease  
331 and arthritis caused by inducible epidermal deletion of Jun proteins. *Nature*.  
332 2005;437(7057):369–75.
- 333 6. Plikus M V, Mayer J, Cruz D De, Baker RE, Maini PK, Maxson R, et al. Cyclic dermal BMP  
334 signaling regulates stem cell activation during hair regeneration. *Nature*. 2008;451(7176):340–  
335 4.
- 336 7. Greco V, Chen T, Rendl M, Schober M, Pasolli HA, Stokes N, et al. A Two-Step Mechanism  
337 for Stem Cell Activation during Hair Regeneration. *Cell Stem Cell*. 2009;4(2):155–69.
- 338 8. Oshimori N, Fuchs E. Paracrin TGF-beta signaling Counterbalance BMP-mediated Repression  
339 in Hair Follicle Stem Cell Activation. *Cell Stem Cell*. 2012;10(1):63–75.
- 340 9. Lee J, Kang S, Lilja KC, Colletier KJ, Scheitz CJF, Zhang Y V, et al. Signalling couples hair  
341 follicle stem cell quiescence with reduced histone H3 K4/K9/K27me3 for proper tissue  
342 homeostasis. *Nat Commun*. 2016;7:11278.
- 343 10. Glitzner E, Korosec A, Brunner PM, Drobits B, Amberg N, Schonthaler HB, et al. Specific  
344 roles for dendritic cell subsets during initiation and progression of psoriasis. *EMBO Mol Med*.  
345 2014;6(10):1312–27.
- 346 11. Stöckl J, Vetr H, Majdic O, Zlabinger G, Kuechler E, Knapp W. Human major group  
347 rhinoviruses downmodulate the accessory function of monocytes by inducing IL-10. *J Clin*

Journal Pre-proof